Mining, Metallurgy & Exploration (2024) 41:3609–3640
https://doi.org/10.1007/s42461-024-01071-6

Mineralogical Impact on the Compaction of Residual Gabbro Soils in the Construction of Platinum Tailings Storage Facilities

Jason Tunnell[1,2] · **Matthys Alois Dippenaar**[1]

Received: 28 April 2023 / Accepted: 21 August 2024 / Published online: 30 September 2024
© The Author(s) 2024

Abstract
Over the past decade, there have been 45 tailings storage facility (TSF) disasters worldwide resulting in fatalities, serious environmental damage, and the destruction of entire ecosystems. These failures often stem from substandard design or operational practices. Many TSFs are constructed in regions associated with intrusive mafic rocks such as gabbro, norite, pyroxenite, and anorthosite, which are commonly found alongside platinum group metals in areas like the Bushveld Igneous Complex in South Africa and the Great Dyke in Zimbabwe. The stability of these structures can be significantly influenced by the residual soils present at the construction sites. Residual soils, both cohesive and non-cohesive, contain varying quantities of different minerals, which can impact the compaction characteristics and, consequently, the stability of the TSF foundations. Cohesive soils rich in clay minerals, such as kaolinite and smectite, exhibit properties that can hinder effective soil compaction. The expansive nature of smectite due to its ability to absorb large amounts of water and host free exchangeable cations counteracts the compaction process, reducing soil stability. Soil compaction is a complex process influenced by several factors, including compaction effort, method, water content, particle size distribution, and mineralogy. This study aimed to analyse these factors using a series of laboratory tests, including foundation indicators, MOD AASHTO compaction testing, and X-ray diffraction analysis, on residual soils from two TSF construction sites. The findings revealed that soils with high clay content tend to retain more water and have a higher optimum water content, adversely affecting their compaction properties. This study highlights the critical need to consider the mineralogical composition and weathering effects of residual soils in the design and construction of TSFs. By improving our understanding of these factors, we can enhance the stability of TSF foundations, reducing the likelihood of future failures. The insights gained from this research highlight the importance of thorough geotechnical assessments in the successful design and maintenance of TSFs.

Keywords TSF · Soil compaction · Residual gabbro · Mineralogy · Great Dyke · Bushveld Igneous Complex

1 Introduction

Tailings storage facilities (TSFs) are a vital part of many mining operations around the world as they provide a means of storing processed waste material that could be detrimental to the environment. Tailings are the waste products produced when extracting valuable minerals or metals from rock ore such as platinum, copper, gold, and uranium to name a few. Mechanical and chemical processes are used to break down ore into a fine sand to extract these valuable commodities. All the unrecoverable and uneconomic remnants (gangue) from this process are waste, and they include chemicals such as cyanide, mercury, and arsenic, as well as finely ground rock particles and contaminated water [1]. A recent study conducted by Piciullo et al. presented a statistical analysis of tailings dam failures since 1915. Through their research, they determined the leading causes of tailings dam failures globally (Fig. 1) [2].

Historically, foundation failures are one of the leading causes of tailings dam catastrophes around the world accounting for at least 16% of all failures recorded. Compaction of in situ material to its maximum dry density is imperative to ensure the foundation stability of these mega structures. The construction of tailings dam foundations is a complex and expensive process that includes the preparation

✉ Matthys Alois Dippenaar
matthys.dippenaar@up.ac.za

[1] Department of Geology, University of Pretoria, Pretoria, South Africa

[2] Fugro Middle East, X42G+J5W, Jebel Ali Freezone Extension, Dubai, United Arab Emirates

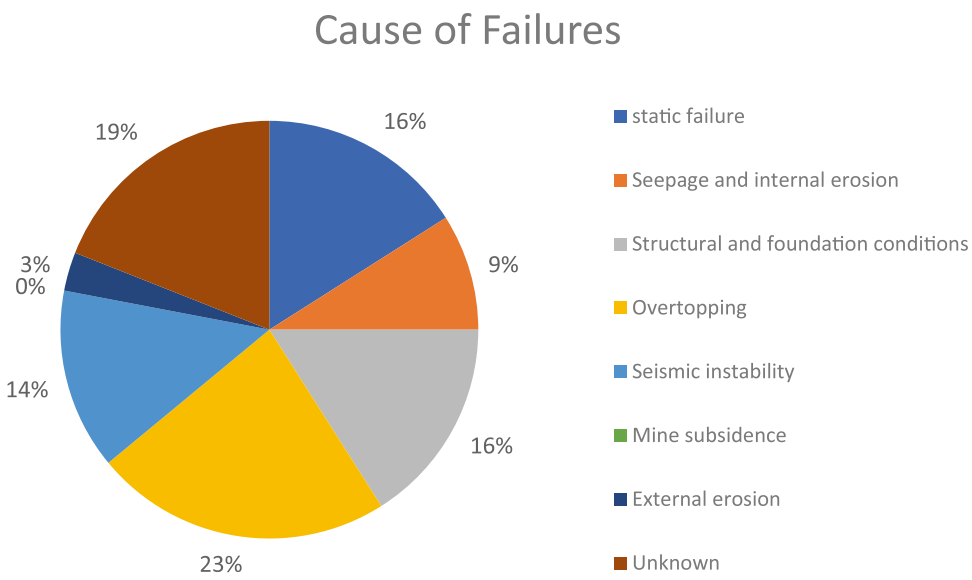

Fig. 1 Causes of tailings dam failures since 1915 [2]

of in situ ground material, the construction of drains and stability bunds, and the placement of high-density polyethylene (HDPE) liner to prevent the contaminated water from infiltrating into the groundwater system.

To lower the costs during construction, in situ material is often used as aggregate for concrete or fill for foundations and earth structures. Rocks such as gabbro and anorthosite, and their residual soils are often used in the construction of these super structures, and as such the importance of understanding these geological units and their engineering properties are important in assuring their stability.

Platinum (Pt) is a dense, malleable, precious metal that is highly inert and is regarded as a noble metal due to its exceptional corrosion resistance. It forms part of the platinum group metals (PGMs) together with palladium (Pd), rhodium (Rh), ruthenium (Ru), iridium (Ir), and osmium (Os). Platinum is one of the most valuable metals on Earth, and it is an important economic mineral that is utilised in various industries such as dentistry, jewellery manufacturing, catalytic converters, and the manufacturing of various medications to treat cancer. Five countries account for approximately 97% of total global platinum production [3]. Table 1 shows the known distribution of platinum reserves across the world.

Due to the abundance of platinum group metals (PGMs) in intrusive mafic rocks located in places like Zimbabwe's Great Dyke and South Africa's Bushveld Igneous Complex, mining operations have extracted large amounts of material from the ground, creating waste and necessitating the construction of more tailing's storage facilities.

The investigation presented here is a study of the importance of mineralogy with specific reference to its effect on the compaction of residual soils derived from gabbroic parent material during the construction of TSF foundations on

Table 1 World platinum reserves [3]

Country:	Reserves (metric tonnes)	World total reserves:
South Africa	110,000	68%
Russia	25,000	16%
Zimbabwe	11,000	7%
Canada	7200	4%
USA	3650	2%
Total of all other countries	3800	2%
World total	**161,000**	**100%**

two platinum-producing mines located in South Africa and Zimbabwe. The research can be used to aid both the design and construction portions of the Global Industry Standard on Tailings Management (GISTM) requirements.

A discussion of the literature pertaining to compaction and its controls are on tailings dam foundations is presented. Physical and chemical properties of specific minerals that could potentially affect compaction were identified based on available literature and specific laboratory testing. This contributes to the understanding of mineralogical controls on compaction that links clearly to this study's research problem.

2 Literature Review

2.1 Overview

In the last decade, approximately forty-five (45) TSF failures have been recorded across the world and the number

of failures is increasing [2]. Failures occur due to various reasons, including poor construction or operation errors resulting in loss of life, major environmental degradation, and the destruction of entire ecosystems [4]. Figure 2 shows the number of recorded tailings dam failures for each prevailing decade.

TSF failures can result in toxic waste material travelling hundreds of kilometres, contaminating rivers and lakes, and killing flora and fauna by flooding land with poisonous slurry. The 2019 collapse of the Brumadinho Dam in Mina Córrego do Feijo (Minas Gerais, Brazil) is an example of how disastrous such occurrences may be. Around 10,000,000 m^3 (ten million cubic metres) of mine waste were spilled into the valley due to the incident. As the slurry moved downstream, it killed 270 people and severely harmed the environment, other ecosystems, and nearby communities (Fig. 3) [2].

Following the failure of the tailings storage facility at Vales Corrego de Feijao Mine in Brumadinho, the Global Industry Standard on Tailings Management (GISTM) was launched on 5 August 2022. According to Clarkson and Williams (2020), a significant tailings storage facility breach might have a cost of between $750 million and $56 billion (social and environmental) [2].

There is a significant risk posed by tailings facility failures to the environment and communities. A dataset including 1743 tailings facilities provided insight into, for instance, construction method, stability, fault

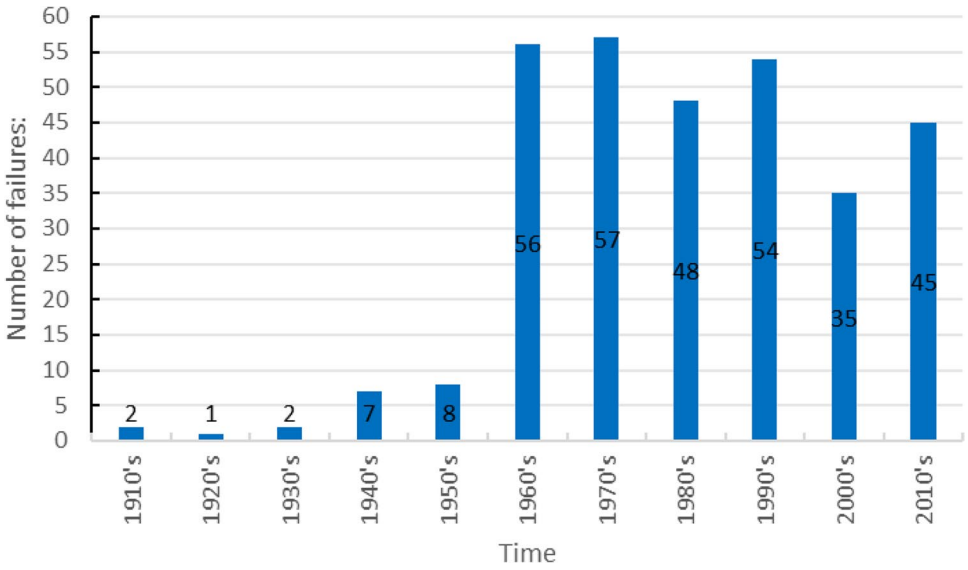

Fig. 2 Tailings storage facility failures to date [4]

Fig. 3 Collapse of the Brumadinho dam in Mina Córrego do Feijo [2]

consequences, and stored volumes. Ten percent of tailings report notable stability failure or concerns sometime in their history. It showed distinct trends according to construction method, governance, age, height, volume, and seismic hazard. Upstream facilities report a higher incidence of stability issues. In-pit/natural and dry-stack facilities, on the other hand, report lower stability issues. All these stabilities are still significant by engineering standards (2%) necessitating careful facility management and governance [2].

Point III of the GISTM in Fig. 4 calls for an improvement in the requirements during the design, construction, operation, and monitoring of tailings storage facilities around the world [5].

TSFs pose global risks to the environment and communities and limited data is available about global risk distribution of facility characteristics that are needed for proper governance. A study conducted by the Church of England found that 687 of a total of 1700 dams (±40%) investigated were deemed high risk. They found that the construction

Fig. 4 Global industry standard on tailings management [5]

method is important because it can be indicative of a dam's level of risk. Their findings are that [6]:

- Upstream facilities pose a higher incidence of stability issues that are elevated in highly built governance settings.
- A lower incidence of stability issues occurs in pit/natural landform and dry-stack facilities, but still significant by engineering standard, so it is important for facility management a governance.

Figure 5 shows the distribution of construction methods for the above-mentioned tailings storage facilities.

2.2 Construction

The construction of tailings storage facilities is a complex and expensive process. These facilities are some of the largest earth structures that geotechnical engineers construct. Due to their vastness, and instead of constructing a fully operational facility with a greater capacity, intermediary retaining embankments are often built utilising the coarse fraction of the tailings further increasing the dam's height and therefore capacity [6]. Once the initial foundation is completed, there are three ways to raise the embankments, namely upstream construction method, downstream construction method, and centreline construction method (Fig. 6). The type of construction used in designing tailings dams is influenced by a variety of factors, including site-specific conditions, safety considerations, cost, and regulatory requirements [7].

2.2.1 Upstream Construction

This is the least costly method of construction due to the minimal amount of material needed for both the initial construction and succeeding raises. The decrease in cost is however at the cost of stability as more of the embankment is underlain by fine tailings as the dam rises. They are extremely vulnerable to liquefaction when the tailings

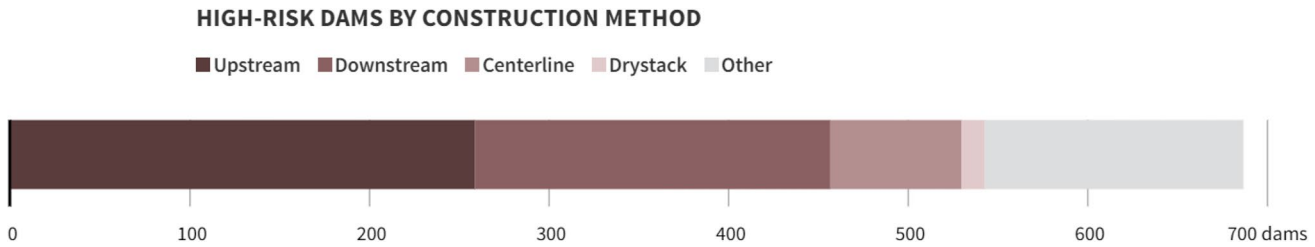

Fig. 5 High-risk dams by construction method [6]

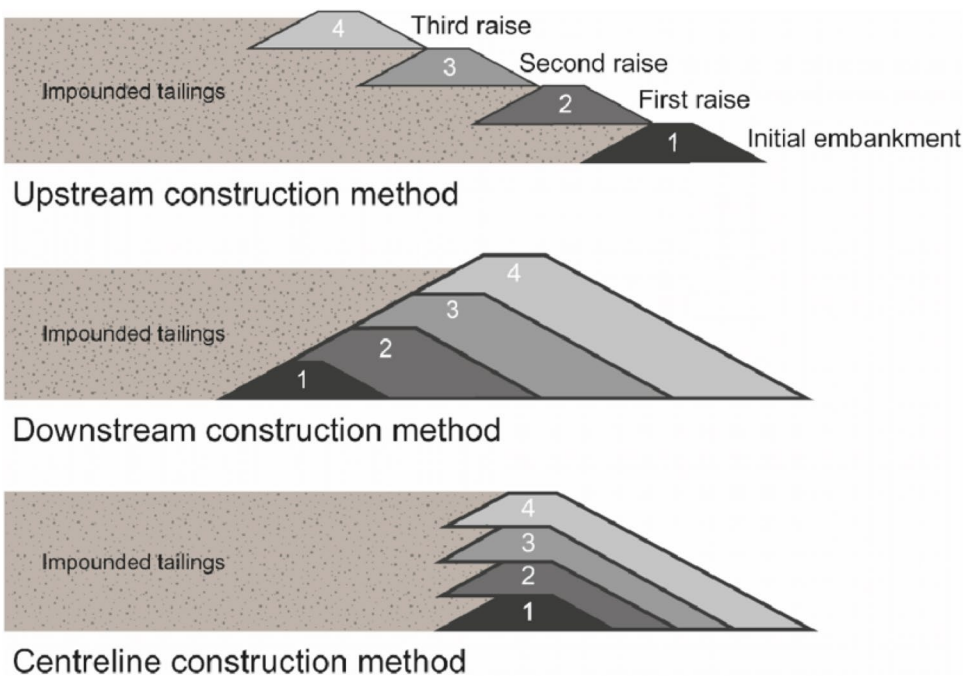

Fig. 6 Tailings dam embankment construction methods [7]

behind the dam wall become saturated with water. The liquid mixture slowly erodes the structure of the dam wall and increases the likelihood of a rupture [7].

2.2.2 Downstream Construction

This method decreases the chance of failure due to breaching as it is more structurally stable because no wet tailings are stored below the embankment. It is also the costliest construction method due to the increased footprint size and amount of material required for construction [7].

2.2.3 Centreline Construction

In terms of output and price, this is a middle-range solution. With this technique, as the tailings dam is raised, the centre lines of the embankments coincide [7].

Due to the continually increasing capacity of the tailings dam, it is imperative that the foundation be constructed appropriately to sustain the ever-increasing load exerted from the expanding dam above. Soil compaction is utilised to increase the bearing capacity and shear strength of the TSF's foundation and initial embankments to increase its stability [7].

2.3 Soil Compaction

Soil compaction is the mechanical densification of soil that involves pressing soil particles together and removing the air between them. It is critical in the broad science of geotechnical engineering, and it plays an important role in all types of geotechnical investigations. Compacted soils are widely used in the construction of geotechnical and geoenvironmental structures, and their durability and stability are directly related to proper soil compaction. The principal soil properties affected by compaction include settlement, shearing resistance, water movement, and volume change [8].

It is an essential activity in civil engineering as it is utilised to create a stable work surface for various construction operations by increasing the shear strength of the underlying geological media. Compaction is commonly used in various projects such as:

Soil compaction can be defined as the process of densification and void ratio reduction in a geological medium that changes hydromechanical properties such as permeability, strength, and porosity [9]. When soil is required to be subjected to a load, soil compaction is generally employed to reduce any potential settlement, and compaction can result in increased shear strength, bearing capacity, void space reduction, permeability reduction, and, ultimately, increased stability [10].

2.4 History of Compaction

Prior to 1830, road construction consisted of merely laying down material and pavers, followed by minimal compaction. The invention of a horse-drawn roller in France in the 1830s revolutionised road construction and brought the first use of mechanical compaction. Steam rollers were introduced in the 1860s, enabling greater degrees of compaction [11]. These advancements in mechanised compaction made it possible to achieve higher degrees of compaction during the construction of highways, dams, and the footprints of structures to prevent settling.

During the 1920s and early 1930s, a study conducted by the California Highway Department revealed that differential settlement owing to uneven amounts of compaction was the leading cause of road failure. This study resulted in the development of the Proctor compaction curves (Fig. 7) for compaction specification [12] and the California Bearing Ratio (CBR) (Fig. 8) which are still being used in laboratory testing today [11].

Various methods have been devised in the past to determine the level of compaction obtained in the field as well as the maximum dry density and optimal moisture content of a soil under laboratory conditions. These laboratory tests serve as benchmarks against which in situ test results can be compared to ensure that the material has been compacted properly. This section will give an overview of the possible laboratory and field experiments that could be used to determine compaction.

2.5 Laboratory Testing

The Standard Proctor Test AASHTO T99 is a lab-based moisture-density relationship test. It serves as a benchmark against which field testing can be evaluated, with all field results represented as a percentage of laboratory results. This makes it easy for a designer to specify what is needed for compaction and to determine whether the material being compacted requires more water or less water to achieve its optimal moisture content (OMC) and, as a result, its maximum dry density (MDD) [15].

The Modified Proctor Test (AASHTO T180) was developed following the need for higher weights to be accommodated on roadways and foundations as technology advanced. This allowed for a larger compaction effort whilst maintaining a lower OMC as the test methods for a modified proctor are identical to those for a proctor, but with slight differences that result in a higher compaction effort being utilised. The approach chosen is determined by the project's requirements and specifications. Figure 9 shows the general setup for both a standard and modified proctor test [16].

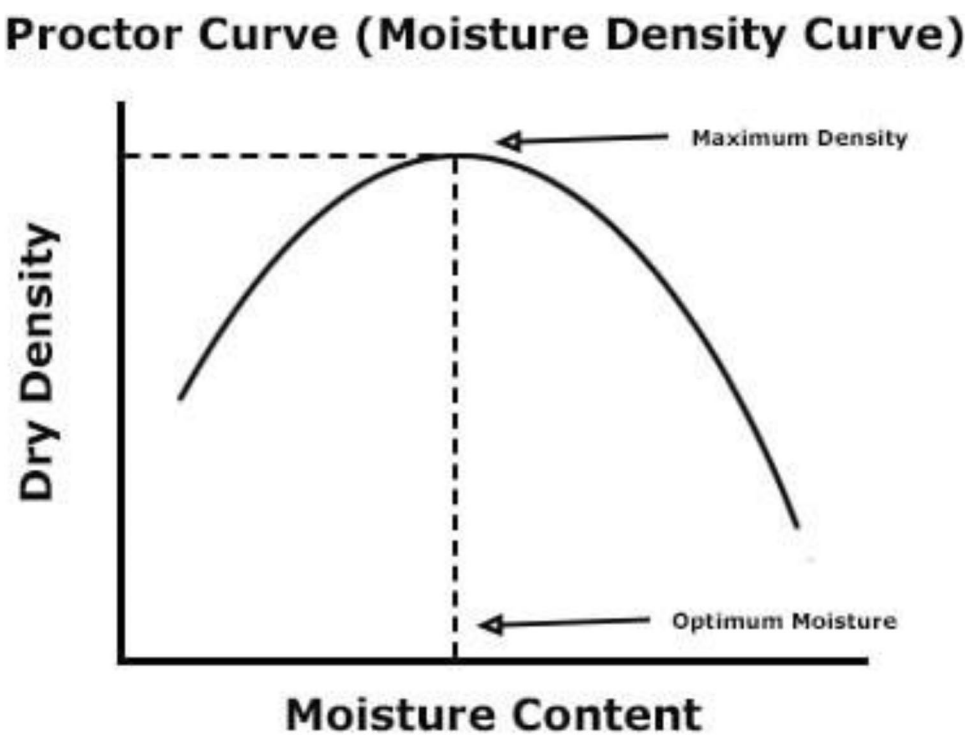

Fig. 7 Proctor compaction curves [13]

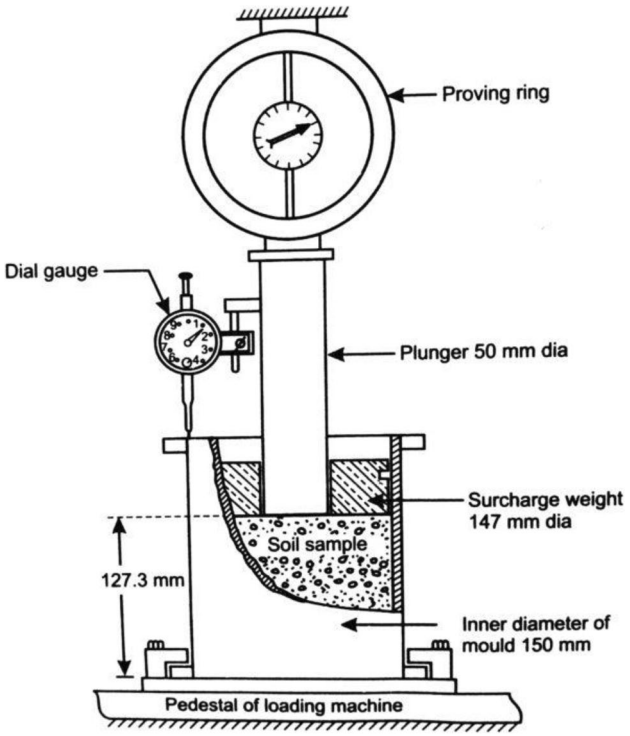

Fig. 8 CBR set up [14]

2.6 In Situ Testing

There are several methods for determining the density and moisture content of soil in situ of which the sand replacement method and Troxler tests are the most utilised tests. The sand replacement setup is shown in Fig. 10 where a small, cylindrical pit is dug in the compacted material to be tested. The soil is removed and weighed, then dried, and weighed again to determine its moisture content as shown in Eq. 1 where M_W is the water mass (kg), M_{TOTAL} is the total mass (kg), and M_S is the soil mass (kg) [17].

$$M_w = M_{total} - M_s \tag{1}$$

A soil's moisture is presented as a percentage of its total mass. The specific volume of the pit is determined by filling it with dry sand of a predetermined density, and the dry weight of the soil removed is divided by the volume of the pit to determine the density of the in situ soil where γ is the dry weight (kg/L), M_S is the soil mass (kg), and V_S is the volume of pit (L) (Eq. 2).

$$\gamma = \frac{M_S}{V_{pit}} \tag{2}$$

This density and moisture content are compared to the maximum dry density and optimal moisture content calculated prior in a lab, which gives us the relative density and moisture content of the material [18].

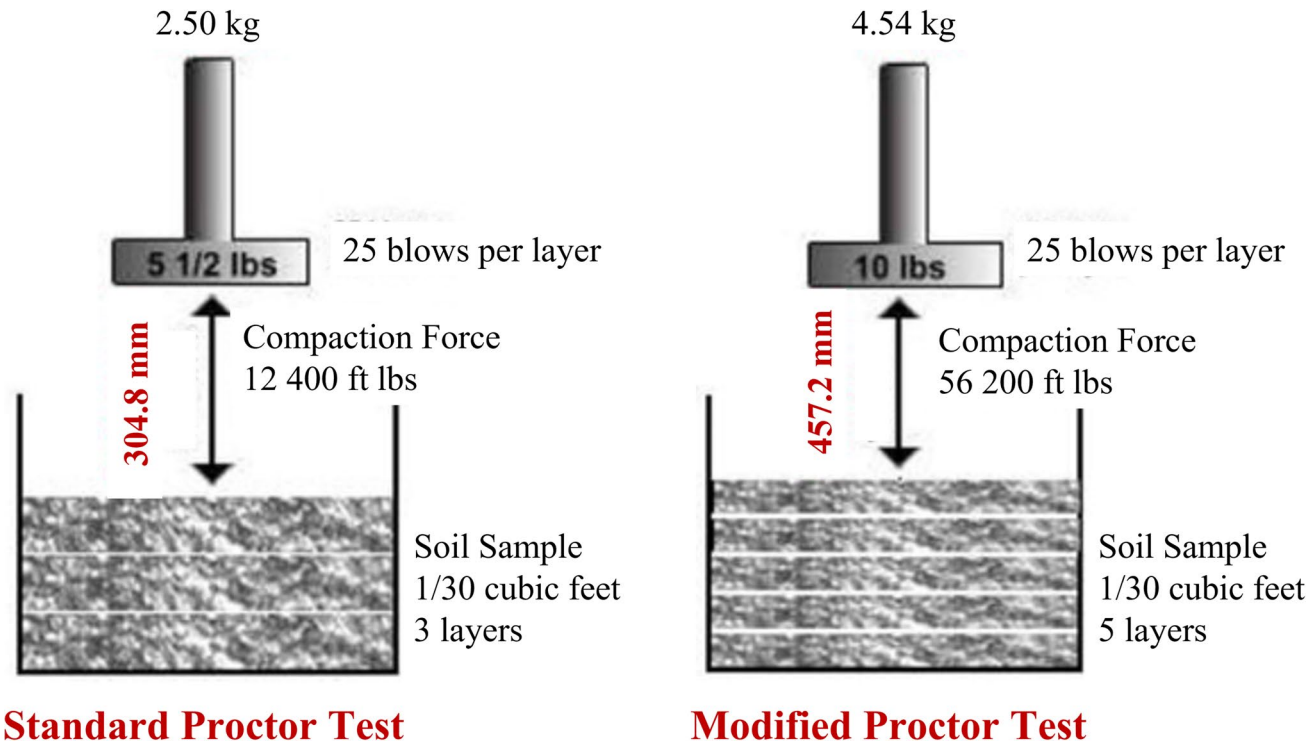

Fig. 9 Standard Proctor Test vs. Modified Proctor Test [14]

Fig. 10 Sand replacement setup [17]

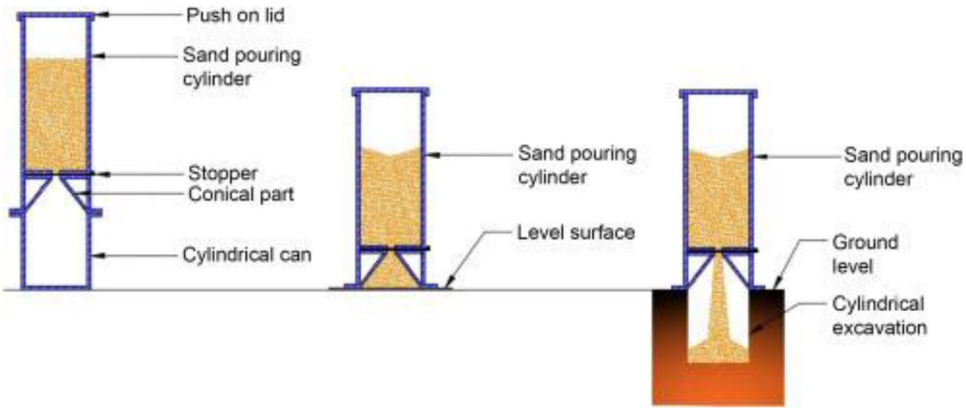

Fig. 11 Nuclear density gauge setup [20]

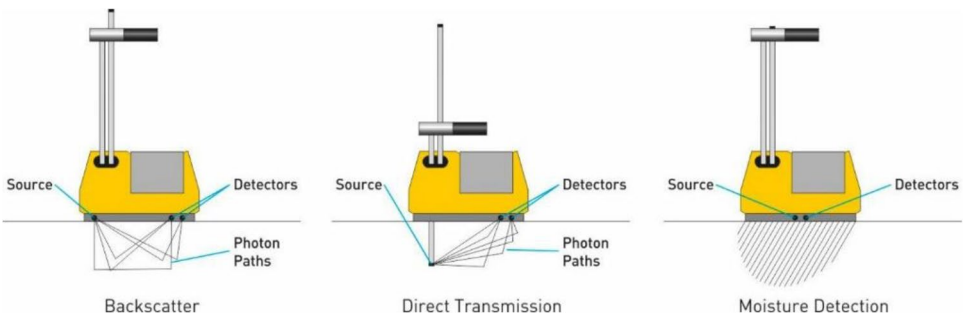

Nuclear density metres are a relatively accurate and fast way of determining density and moisture content (Fig. 11). The device uses a radioactive isotope source caesium 137 at the soil surface in the backscatter method, or from a probe placed into the soil in the direct transmission method. The isotope source releases photons as Gamma rays which radiate back to the detectors on the underside of the unit. Dense soil will absorb greater amounts of radiation than loose soil and the readings are computed to show overall density [16]. Water content can also be determined, but a moisture correction test is usually required for correlation [15].

Tailings constitute mad-made soils remaining from mineral processing and having the same geotechnical properties as all soils, meaning that it can be used for some construction purposes. For the compacted tailings, the opening fracture toughness (plasticity index divided by flow index) component of the soils increases with a decrease in span ratio (span length divided by vertical height), whereas the shear fracture toughness component increases with a decrease of span ratio [19].

2.7 Factors Affecting Compaction

The controlling elements that influence soil compaction can be separated into various internal and external factors. Factors affecting the compaction properties are complex and numerous, including grain composition, aggregate shape, moisture content, rolling technology, and compaction power. However, it is difficult to analyse each factor and understand its mechanism individually [19].

The following factors are addressed, noting that mineralogy will not influence external factors such as the compaction effort and compaction method [21]:

- Compaction effort
- Compaction method
- Water content
- Particle size distribution
- Mineralogy.

2.7.1 Compaction Effort

Increased compaction effort raises the soil's maximum dry density, and as the soil becomes more compacted, the rate of compaction decreases. As the soil densifies soil particles are forced into a denser packing configuration and the porosity decreases, resulting in a lower moisture content as the water dissipates out of the pores. The compaction curves shift to the top left of the graph as the compaction effort increases as shown in Fig. 12. Increasing compaction effort allows a soil to be compacted to its MDD at a lower OMC, and only when the water content reaches its OMC does this effect of increased compaction become evident. After this, the air void volume becomes constant, and the effect of increased compaction effort is not significant [21].

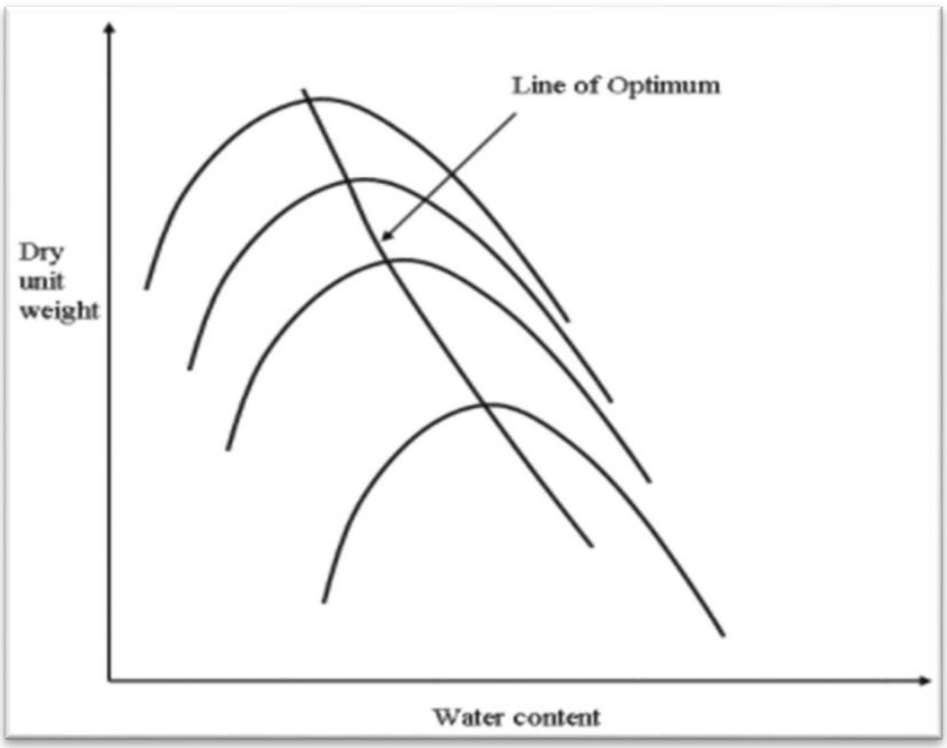

Fig. 12 Effect of compaction effort [22]

2.7.2 Method of Compaction

The method of compaction has an impact on the shape of the compaction curves that are created. Factors such as contact pressure, rolling speed, number of passes, and layer thickness will all affect the compaction effort achieved independent of the machinery used to compact a soil [23]. Machinery that should be utilised for different soil types is provided in Table 2 [19].

Table 2 Machinery used for different soil types [19]

Type of soil	Suggested equipment/machinery
Crushed rock, gravelly sand	Smooth wheel roller
Gravels, sand	Rubber tyred roller
Sands, gravel, silty soil, clayey soils	Pneumatic tyred roller
Silty soil, clayey soil	Sheep foot roller
Soils in confined zone	Rammer
Sands	Vibratory roller

2.7.3 Water Content

Water content plays a significant role in compaction characteristics of soil. At low water contents (below OMC), soil is stiff and has a higher resistance to compaction. As the water content increases, a film of water forms around soil particles and acts as a lubricant allowing particles to slide past one another. This results in the soil being compacted with more ease into a dense packing configuration (Fig. 13). At OMC, soil reaches its maximum unit weight, and with further addition of water, it displaces the soil particles and lowers its ability to be compacted. This results in a decrease in unit weight as the water particles replacing the soil particles have a lower unit weight and negatively affect the sample's ability to be compacted [24].

Water-holding capacity is controlled predominantly by soil texture and the presence of organic matter. Soils with smaller particles (silt and clay) have larger surface areas than those with larger particles (sand and gravel), and a large surface area allows a soil to hold more water due to increased adhesion. This means that soils with higher levels of organic material and higher silt and clay fractions have a higher affinity to water and therefore have a higher water-holding capacity [26].

Soil texture influences water holding capacity, and the type of clay also affects the soil's water holding capacity. 1:1 layered silicate minerals such as kaolinite (Fig. 14a) have one tetrahedral sheet of silica bonded to one octahedral sheet of alumina. The bond between the tetrahedral sheet and octahedral sheet forms through hydrogen bonding and is relatively strong. 2:1 layered minerals can be separated into two different categories, namely 2:1 non-expanding clays such as illite (Fig. 14b), and 2:1 expanding clays such as montmorillonite (Fig. 14c) which are known for their interlayer expansion which happens during their swelling behaviour when they are wet [27].

These layered silicates consist of one octahedral sheet sandwiched in between two tetrahedral sheets. Oxygen atoms occur on the top and bottom of the tetrahedral sheets of two adjacent units exhibit a slight attraction to one another. As a result, there is a variable space between the layers that is occupied by water and exchangeable cations held together by Van der Waals forces, causing water and exchangeable cations to readily enter the interlayer gap, and layers to expand. Paired with the greater surface area of clay minerals, this interaction can result in swelling and increased pore pressure that further detriments compaction. The ideal structure of kaolinite has no charge resulting in a fixed structure and very little to no swelling when interacting with water. The presence of 1:1 layered silicate minerals in a soil will result in a higher OMC due to the smaller particle size, and therefore greater surface area for atmospheric water to bond [28].

2.7.4 Particle Size Distribution

The compaction of a soil is strongly influenced by its composition. There are implicit relationships between the particle size distribution (PSD) and the physical and mechanical properties of granular materials, even though these qualities are exceedingly complex and challenging to ascertain [29]. Coarse-grained soils can be compacted to a higher dry density than the fine-grained soils, and if the quantity of fines is raised above what is required to fill voids in coarse-grained soils, the maximum dry density drops, and therefore, a well-graded soil has a significantly higher dry density than a poorly graded soil. Cohesive soils, such as heavy clays, clays, and silts, are more resistant to compaction because their maximum dry density is lower.

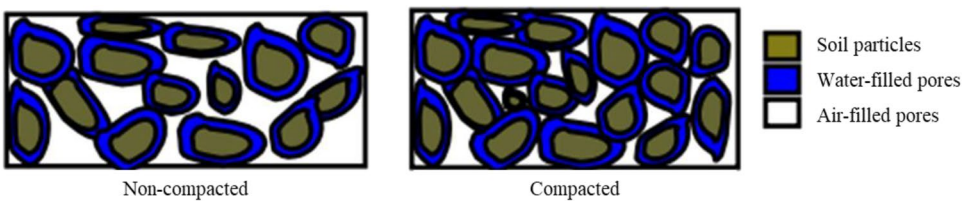

Fig. 13 Water content of compacted vs. non-compacted soil [25]

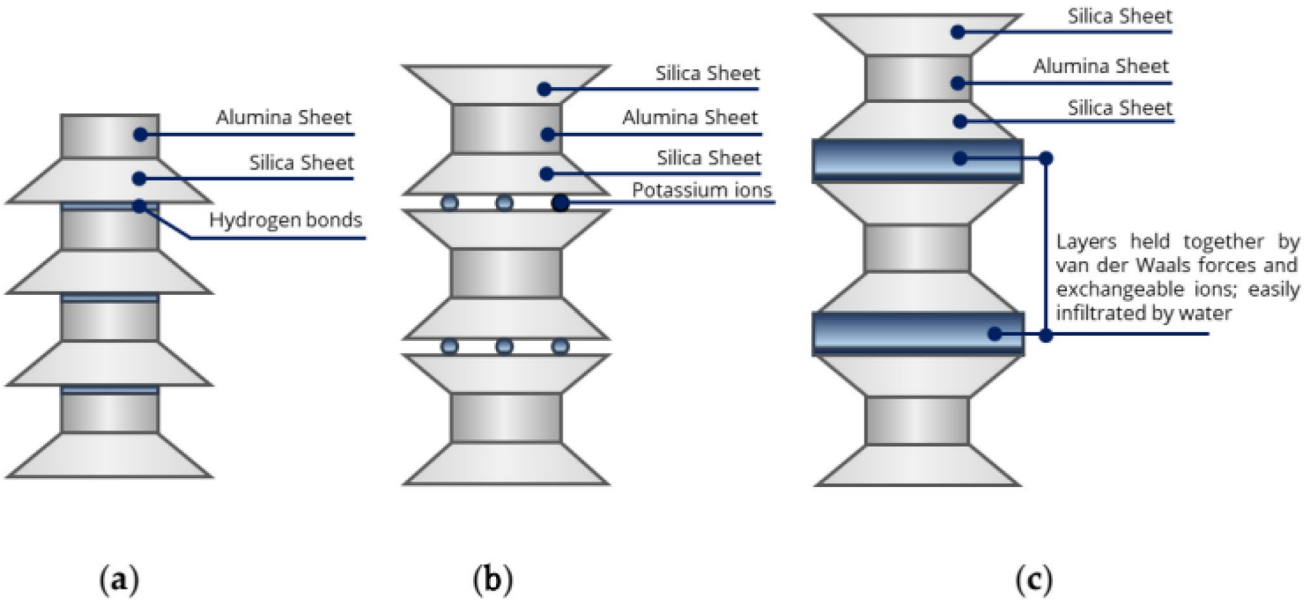

Fig. 14 (**a**) 1:1 clay minerals such as kaolinite, **b** 2:1 clay minerals such as illite, and **c** 2:1 clay minerals prone to expansive behaviour such as montmorillonite [27]

Sandy soils and gravelly soils have little cohesion and are susceptible to easier levels of compaction. The varying shape of minerals present in a soil will affect its ability to be compacted into its densest packing formation and can therefore affect its maximum dry density. The effect of the gravel content of a soil together with soil grading and index properties play a vital role in the soil's ability to be compacted. The increasing gravel content in a sample will also increase its maximum dry density and lower its OMC [30].

2.8 Mineralogy

Although mineralogy is not generally described as an influencing factor on compaction, it is considered as being the main controlling factor for compaction. The mineralogy of parent material is imperative in the formation of residual soils as it determines what minerals are available and subjected to alteration [31]. The secondary minerals formed in a soil will determine the physical and chemical properties of the geological media.

The clay mineralogy of residual soils compared by Alcott showed a correlation between the clay fraction of a soil and its compaction characteristics using regression, finding that the fines fraction of a soil is more likely to negatively affect its compactability than its coarse fraction [30]. Moisture content and particle size have been identified as critical internal controls. Due to their water holding capacity and generally reduced MDD, soils containing substantial concentrations of clay mineralogy are less susceptible to compaction and more likely to have a reduced shear strength. Many soils contain phyllosilicates (clay minerals) that dominate the clay fraction, and their presence affects the soil's physical, physical–chemical, water-physical, physical–mechanical properties (plasticity, stickiness, swelling, shrinkage, cohesion), and structure and moisture retention [32].

3 Site Description

3.1 Site Localities

Two sites were identified for this. The Mareesburg Tailings Storage Facility (MTSF) lies within the Der Brochen Project Area approximately 25 km south-west of the town of Steelpoort and 40 km west of the town of Mashishing in the Limpopo Province in South Africa. The Selous Metalogical Complex (SMC) TSF expansion site is located approximately 4 km northwest of the town of Selous in the Mashonaland West Province of Zimbabwe. The locality of both sites is shown in Fig. 15.

The data and information used for this study was obtained during fieldwork and reporting of SRK Consulting Projects.

The MTSF is being constructed in multiple phases. The purpose of the phased construction approach is to allow deposition of tailings in the phase 1 area of the dam whilst construction continues of the following phases. Fig. 16 shows an aerial photograph of the MTSF with deposition occurring in the phase 1 area (grey from tailings) whilst construction of phase 2 and phase 3 is ongoing.

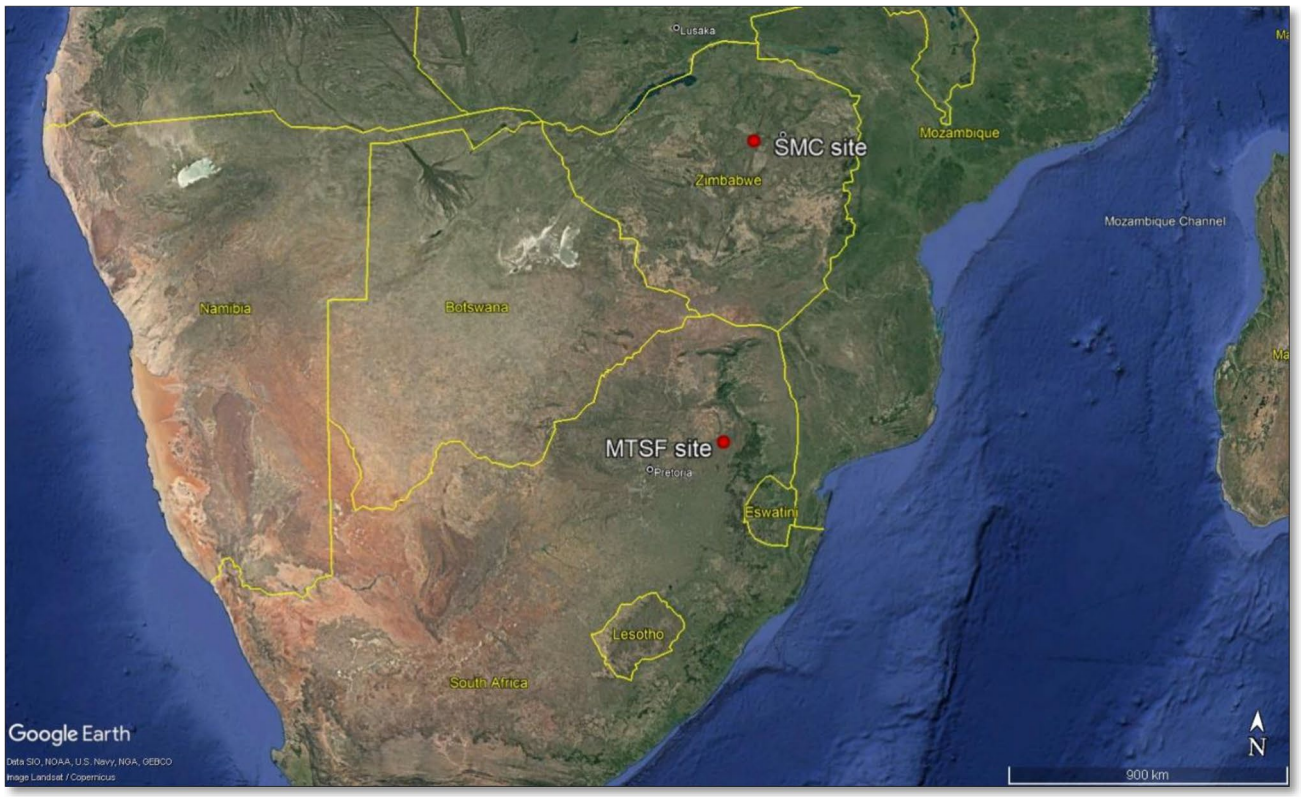

Fig. 15 Site locality map (© Google Earth, 2022)

Fig. 16 Mareesburg TSF ongoing construction

The Selous Metallurgical Complex (SMC) currently processes ore from several different portals across the Great Dyke of Zimbabwe. This results in copious amounts of waste in the form of tailings that needs to be stored resulting in the existing TSF being near capacity (Fig. 17). Construction of a new facility commenced in January 2022 to take over deposition when the existing dam is at capacity.

The MTSF site is characterised by an average annual temperature of 22 °C and an average annual rainfall of 52 mm, and the SMC site is characterised by an average

Fig. 17 Selous metallurgical complex existing tailings dam

annual temperature of 28 °C and an average annual rainfall of 48 mm [33] as shown in Table 3.

3.2 Geology

The Bushveld Igneous Complex, which formed approximately 2.1 Ga (billion years) ago in northern South Africa, is the world's largest mafic layered intrusion and contains more than half of the world's known platinum group metal (PGM) reserves. It is subdivided into, from the oldest to the youngest, the Rustenburg Layered Suite, the Lebowa Granite Suite, and the Rashoop Granophyre Suite. The Pretoria Group of the Transvaal Supergroup and the Rooiberg Group generally underlies it [34]. The Rustenburg Layered Suite contains mainly mafic rocks and is divided into several different stratigraphic units that are rich in PGMs that is associated with many mining operations. Figure 18 shows various mining operations constructed across the Bushveld Igneous Complex for the extraction of these rare earth metals.

The Mareesburg TSF area is underlain by alternating sequences of leucocratic and more melanocratic igneous rocks of the Dwarsrivier Subsuite (Vdr) and Shelter Norite (Vsn) of the Rustenburg Layered Suite of the Bushveld Igneous Complex (BIC) as shown in Fig. 19. These rocks are characterised by medium grained anorthosite, norite, and gabbro, and they host the Merensky Reef pyroxenites, and Upper Group (UG) and Middle Group (MG) chromitite zones [34].

The Steenkampsberg Formation (Vsq) quartzite and subordinate shale (Pretoria Group, Transvaal Supergroup) is present in the far eastern regions of the area and occur along the intrusive contact between the older Transvaal Supergroup lithologies and the younger Bushveld Igneous Complex rocks [35].

The SMC TSF site lies on the Great Dyke of Zimbabwe (Fig. 20) which is a layered mafic to ultra-mafic igneous intrusion into the surrounding Archean granites and greenstone belts of the Zimbabwe Craton. The dyke is composed of two major successions, namely (1) a lower ultramafic succession (up to 2.2-km thick) dominated from the base up by cyclic repetitions of dunite, harzburgite, pyroxenite, and chromitite, and (2) an upper mafic sequence (up to 1.15-km thick) consisting mainly of gabbronorite and gabbro [36].

The Great Dyke of Zimbabwe, which formed approximately 2.5 billion years ago, is unique among large, layered intrusions due to its highly elongate shape. The dyke formed due to the intrusion of a series of linked magma chambers into the surrounding granitoids, schists, and gneisses of the Kaapvaal and Zimbabwe Cratons. During the filling process, the intrusion began as a series of initially isolated chambers that became linked at progressively higher levels [36]. The Selous Metallurgical Complex where fieldwork and sampling

Table 3 Monthly average temperature (°C) and precipitation (mm) of the two sites [33]

Month	Jan	Feb	Mar	Apr	May	Jun	Jul	Aug	Sep	Oct	Nov	Dec
Mareesburg TSF												
Temperature	25	25	24	21	20	18	17	21	24	24	24	25
Precipitation (mm)	117	96	72	34	10	3	3	4	13	61	83	131
Selous Metalogical Complex TSF												
Temperature (°C)	28	28	28	26	26	24	24	28	32	34	32	30
Precipitation (mm)	163	118	79	24	6	1	1	0	1	6	57	125

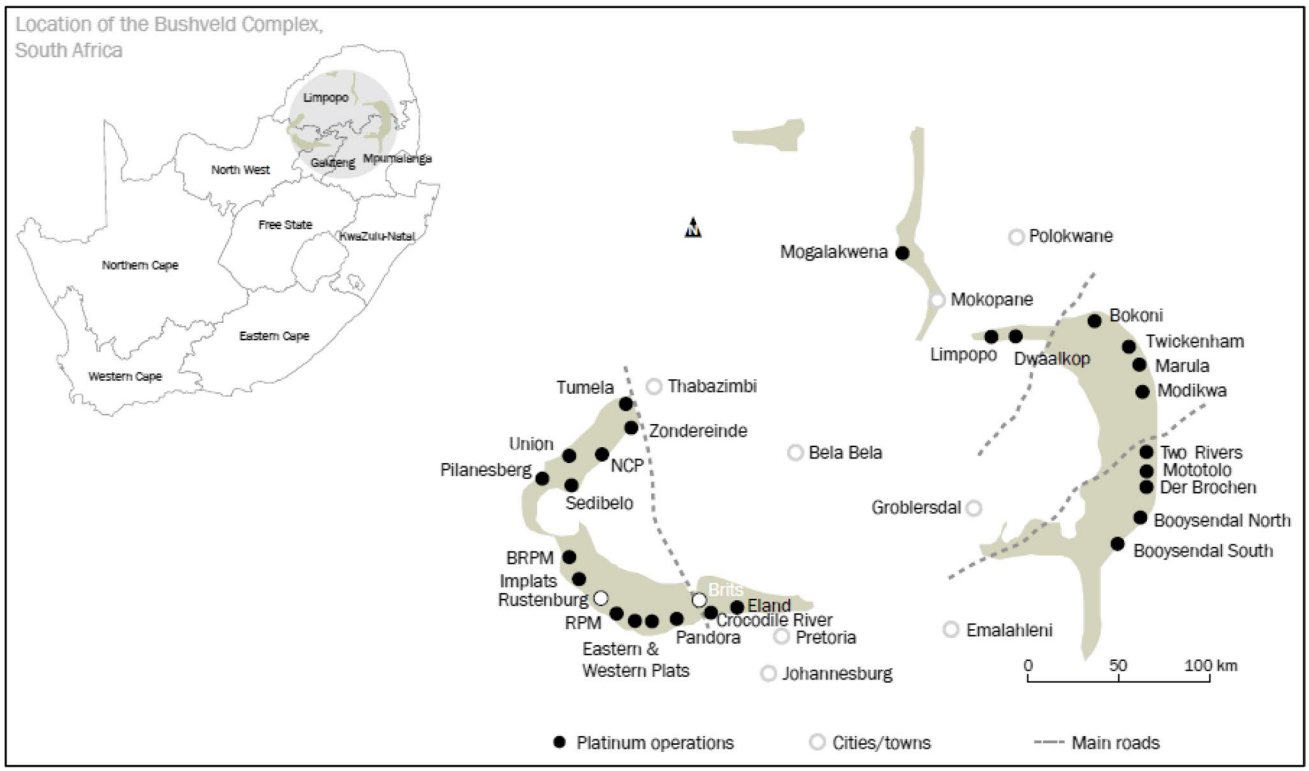

Fig. 18 Platinum mining operations in South Africa [34]

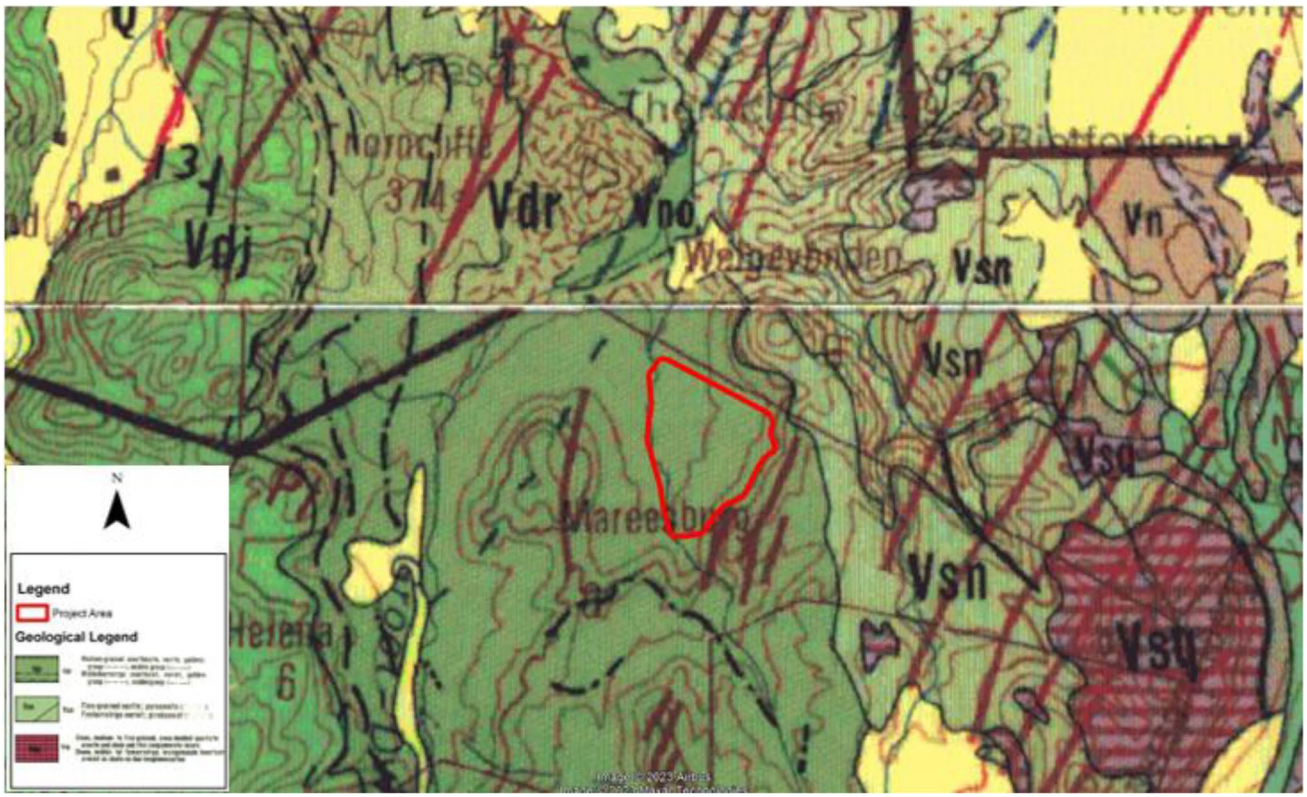

Fig. 19 MTSF geology (1:250 000 2530 Barberton geological map) [35]

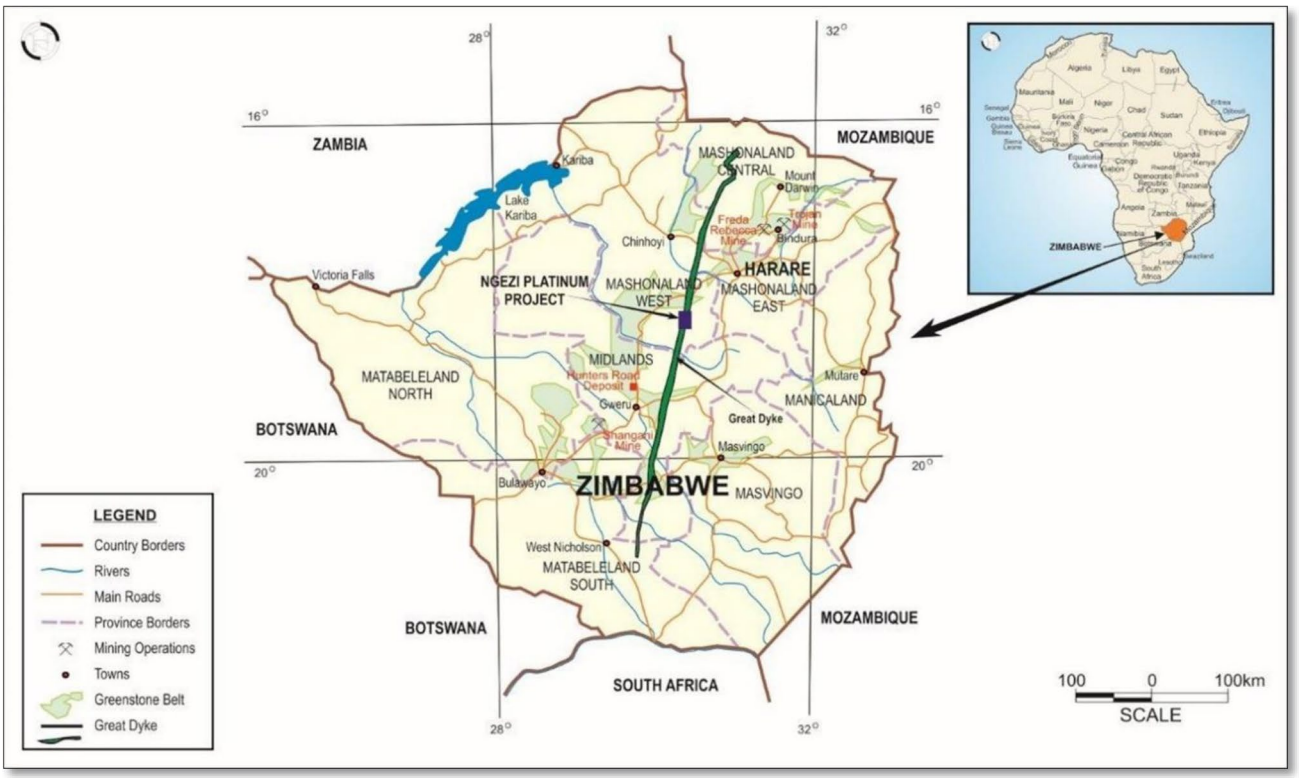

Fig. 20 SMC site geology [36]

were conducted is located on the old Hartley Complex site. Figure 21 shows various mining operations constructed along the dyke for the extraction of rare earth metals.

The sites are underlain by gabbro and gabbronorite. Gabbro, the rock relevant to this study, is an intrusive, mafic, coarse-grained rock with allotriomorphic texture that contains low silica contents and is made up of pyroxene, hornblende, olivine, and Ca-plagioclase [36].

4 Methodology

4.1 Soil Profiling and Sampling

The two sites were visited from 2018 to 2022 during which 65 samples (Table 4) were taken as part of the design phase geotechnical investigations and the construction of the tailing's dams. Samples were divided into cohesive and non-cohesive categories based on relative fines content at the discretion of the engineering geologist in the field, and that were confirmed by the laboratory tests.

Cohesive soils are soils that have cohesive properties due to the presence of fine particles that are primarily clay minerals. These soils are characterised by their ability to stick together and maintain their shape when wet. When they become saturated with water, they become very sticky and plastic making them difficult to work with during construction. Cohesive soils possess high cohesion, which contributes to their ability to resist shearing forces. However, they generally have lower internal frictional strength compared to non-cohesive soils, which more significantly impacts a soil's resistance to shear forces. They are often associated with low permeability which can lead to water retention and slow drainage [37].

Non-cohesive soils are soils that lack cohesive properties, and they are composed of larger particles such as sand, gravel, and sometimes silt. Unlike cohesive soils, non-cohesive soils do not stick together when wet and do not maintain their shape. They rather depend on internal friction and particle interlocking for stability, resisting breaking down when subjected to shear stresses. Non-cohesive soils have a lower proportion of fine particles and do not exhibit plasticity and are therefore generally easier to work with during construction. Non-cohesive soils tend to be well-draining and are less likely to retain water, making them suitable for many construction applications where drainage is important [38]. Silt can be identified and subsequently distinguished from fine sand and clay through various field tests described by Swart et al. [39].

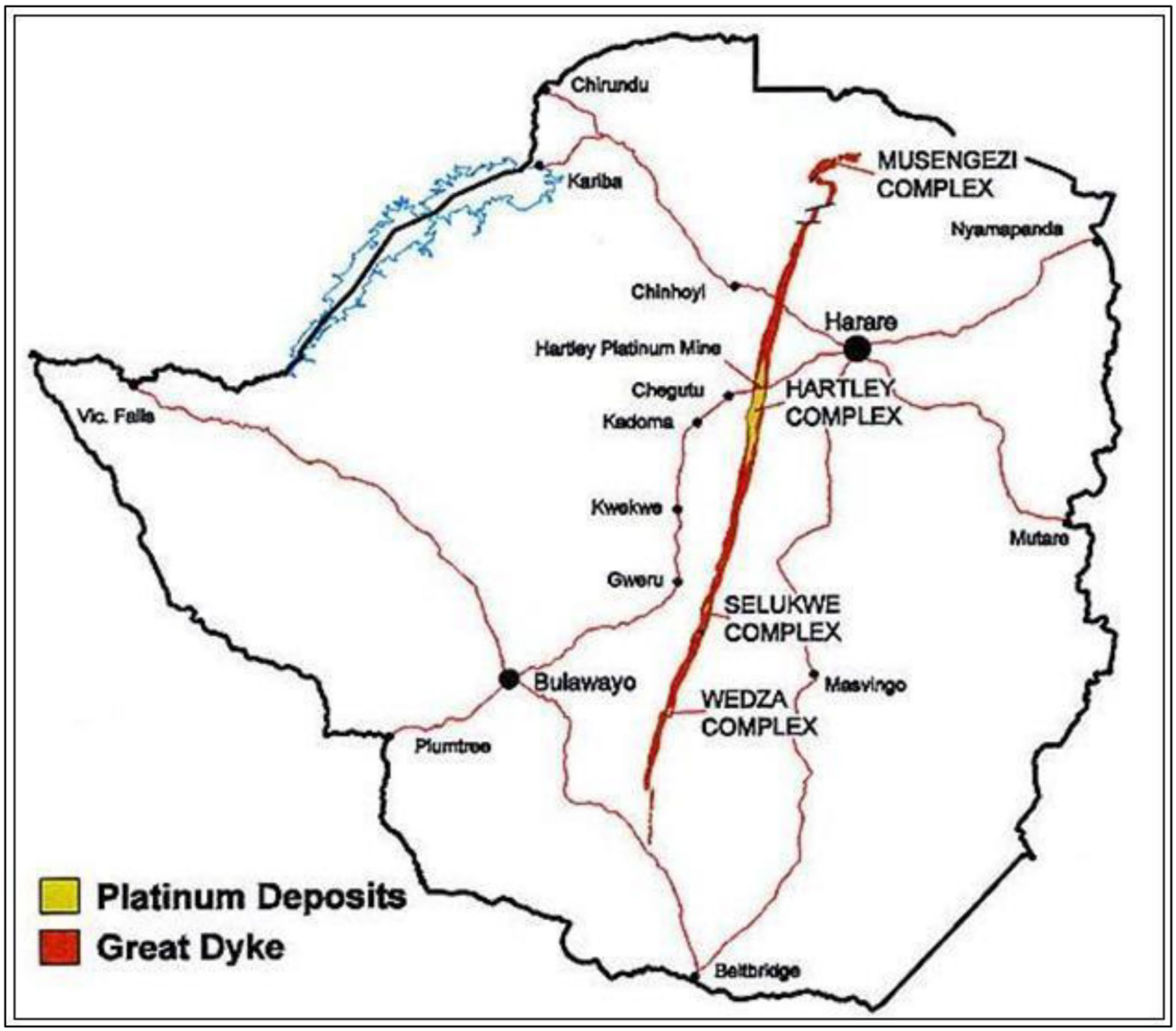

Fig. 21 Platinum mining operations in Zimbabwe [36]

4.2 X-ray Powder Diffraction (XRD)

The mineralogical make-up of the samples was determined at the X-Ray Analytical Facility, University of Pretoria. The samples from each locality were oven-dried, milled, and prepped for testing. The samples were analysed using a Panalytical X'Pert Pro powder diffractometer in θ–θ configuration with an X'Celerator detector and variable divergence, and fixed receiving slits with Fe-filtered Co-Kα radiation ($\lambda = 1.789$ Å). The mineralogy was determined by selecting the best-fitting pattern from the ICSD database to the measured diffraction pattern, using X'Pert High score plus software. The relative phase amounts (weight% of crystalline portion) were estimated using the Rietveld method. Figure 22 shows the equipment and some of the pressed powders.

4.3 Foundation Indicators

Samples taken from the MTSF, and SMC localities were submitted to the relevant laboratories for foundation indicator tests. The results included PSD using sieves for the coarse non-cohesive grain sizes and hydrometer testing for the fine cohesive fraction. It also analysed the moisture content and Atterberg limit according to SANS 3001. All the samples were plotted on a PSD curve and an A-line plasticity graph, and expansiveness was based on Van der Merwe's

Table 4 Sample summary

No.	Site	Test	Sample ID	Date tested
Cohesive residual samples				
1	MTSF	Foundation indicator	SRK-110-1663	03/03/2021
2			SRK-110-1650	03/03/2021
3			SRK-110-1656	03/03/2021
4			SRK-110-1667	03/03/2021
5			SRK-110-1666	03/03/2021
6		MOD AASHTO	S481	24/07/2020
7			S482	24/07/2020
8			S483	24/07/2020
9			S484	24/07/2020
10			S485	24/07/2020
11			S503	25/07/2020
12		X-ray diffraction	MTSF C 01	03/04/2022
13			MTSF C 02	03/04/2022
14			MTSF C 03	03/04/2022
15			MTSF C 04	03/04/2022
16			MTSF C 05	03/04/2022
17	SMC	Foundation indicator	SRK-98-1522	25/08/2020
18			SRK-98-1529	25/08/2020
19			SRK-98-1531	25/08/2020
20			SRK-98-1532	25/08/2020
21		MOD AASHTO	Access road one east (ch2800-2960)	18/05/2022
22			Access road one east (ch2980-3160)	17/05/2022
23			Access road one east sample 2	23/05/2022
24			Access road one east sample 3	19/02/2022
25			Access road one west (ch280-360)	02/04/2022
26			Access road one east (ch280-480)	25/03/2022
27		X-ray diffraction	SMC C 01	15/03/2022
28			SMC C 02	15/03/2022
29			SMC C 03	20/03/2022
30			SMC C 04	20/03/2022
31			SMC C 05	20/03/2022
Non-cohesive residual samples				
32	MTSF	Foundation indicator	SRK-110-1649	03/03/2021
33			SRK-110-1651	03/03/2021
34			SRK-110-1652	03/03/2021
35			SRK-110-1653	03/03/2021
36			SRK-110-1654	03/03/2021
37			SRK-110-1655	03/03/2021
38			SRK-110-1664	03/03/2021
39		MOD AASHTO	SRK-110-1649	03/03/2021
40			SRK-110-1651	03/03/2021
41			SRK-110-1652	03/03/2021
42			SRK-110-1653	03/03/2021
43			SRK-110-1654	03/03/2021
44			SRK-110-1664	03/03/2021
45		X-ray diffraction	MTSF NC 01	26/05/2020
46			MTSF NC 02	26/05/2020
47			MTSF NC 03	26/05/2020
48			MTSF NC 04	26/05/2020
49			MTSF NC 05	26/05/2020
50	SMC	Foundation indicator	SRK-98-1519	25/08/2020
51			SRK-98-1528	25/08/2020
52			SRK-98-1530	25/08/2020
53			SRK-98-1534	25/08/2020
54			SRK-98-1535	25/08/2020
55		MOD AASHTO	Outfall channel berm (ch120-240) 1	04/07/2022
56			Outfall channel berm (ch120-240) 2	04/07/2022
57			Outfall channel berm (ch120-240) 3	20/06/2022
58			Outfall channel berm (ch240-360) 3	20/06/2022
59			Penstock line 1 (ch90-120) 1	03/06/2022
60			Penstock line 1 (ch90-120) 2	03/06/2022
61		X-ray diffraction	SMC NC 01	25/04/2022
62			SMC NC 02	25/04/2022
63			SMC NC 03	25/04/2022
64			SMC NC 04	25/04/2022
65			SMC NC 05	25/04/2022

method [41] that relates the clay content and plasticity index to each other.

4.3.1 Particle Size Distribution (SANS 3001-GR1) [40]

PSD testing was conducted on the samples to determine the percentages of gravel, sand, silt, and clay as per the guidelines in SANS 3001. The PSD information is crucial for designing foundations, determining soil behaviour, and assessing the suitability of the soil for construction projects. The following steps outline the methodology of the PSD test:

- Sample collection: Representative soil samples are collected from the sites where geotechnical investigations are conducted.
- Sample preparation: The collected soil samples are prepared for testing which may involve drying, breaking up clumps, and removing organic material or debris.
- Sieve analysis: Sieve a representative soil sample through a series of sieves with progressively smaller openings separating the soil into different particle size fractions and then measure the mass of soil retained on each sieve.
- Particle size calculation: Plot the particle size distribution on a logarithmic graph showing the percentage passing of soil particles through each sieve size, and include, if needed, the hydrometer analyses to be able to express the particle sizes in terms of gravel, sand, silt, and clay fractions.
- Hydrometer analysis (SANS 3001-GR3): For fine-grained soils, the remaining soil particles from the sieving is dispersed in water, then the settling velocities of the particles is determined using a hydrometer, and finally the particle size distribution is calculated based on the sedimentation data.

4.3.2 Moisture Content (SANS 3001-GR20) [42]

A soil's moisture content is an important parameter that indicates the fraction or percentage of water present in the soil pores and can be presented in terms of volume or weight. The moisture content of a soil sample can be calculated using Eq. 3 and based on the following standard method:

- Weighing the sample: Weigh an empty, clean, and dry container or tin (often referred to as a moisture tin) and record its weight as W_1.
- Adding the soil: Place a portion of the soil sample into the moisture tin ensuring that the amount of soil is suf-

Fig. 22 PANalytical X'Pert Pro powder diffractometer (left) and XRD pressed powder samples (right) (© Jason Tunnell)

ficient to provide a representative sample without it overflowing the tin.

- Recording the combined weight: Weigh the moisture tin with the soil and record its weight as W_2.
- Oven-drying: Place the moisture tin with the soil sample in an oven set to a standard temperature that is typically 105 °C (221 °F) causing the soil to heat and all moisture to be removed. The oven-dried soil reaches a constant weight meaning that there is no further reduction in weight, and this typically means that all moisture has been removed. The process generally takes several hours.
- Recording the final weight: Weigh the moisture tin with the dried soil sample and record its weight as W_3.

$$MC = \frac{W_2 - W_3}{W_3 - W_1} \times 100 \tag{3}$$

4.3.3 Atterberg Limits (SANS 3001-GR10)[43]

The Atterberg limits include the liquid limit (LL), plastic limit (PL), and shrinkage limit (SL) that are used to classify fine-grained soils such as clay and silt. They are important for assessing the behaviour of fine-grained soils, including their potential for shrinkage, swelling, and moisture sensitivity. The Atterberg limits are typically determined through different methods. The chart depicts the samples as a function of the adjusted PI of the whole sample (PI_{ws}) calculated by the PI and by the fraction of the soil that passes the 0.425-mm sieve ($P_{0.425}$) (Eq. 4)against the clay percentage of each sample (54).

$$PI_{WS} = PI \times \left(\frac{P_{0.425}}{100} \right) \tag{4}$$

Liquid limit (LL):

- Take a representative soil sample, ensuring that it is free from large particles and contaminants.
- Air-dry the soil sample and pass it through a 425-µm sieve.
- Mix the soil with distilled water to form a uniform paste.
- Place a portion of the soil paste into the cup of the Casagrande apparatus.
- Level the soil surface in the cup with a spatula or grooving tool.
- Use the grooving tool to cut a groove along the centreline of the soil paste.
- Rotate the handle of the Casagrande apparatus at a rate of two revolutions per second until the two halves of the soil come into contact at the bottom of the groove for a length of 13 mm (1/2 inch).
- Record the number of blows (N) required for the soil to close the groove.
- Repeat the procedure with different moisture contents to obtain a range of blow counts (typically 10–40 blows).
- Calculate the liquid limit using the number of blows and the calibration chart for the specific device used.

Plastic limit (PL):

- Air-dry the soil sample and pass it through a 425-µm sieve.
- Mix the sieved soil with distilled water to form a uniform paste and the soil should be moist enough to roll into threads without sticking to your hands excessively.
- Take a small portion of the moist soil and form it into an ellipsoidal mass and roll the mass between your fingers and a smooth, hard surface until a diameter of approximately 3 mm is achieved.

- The moisture content of the soil paste at this point is the plastic limit.

Shrinkage limit (SL):

- Take another portion of the soil paste that was used for the liquid and plastic limit tests.
- Form a small, flat, and thin soil specimen.
- Place the specimen in an oven and dry it until there is no further reduction in size.
- Measure the moisture content of the soil specimen after drying, and this moisture content is the shrinkage limit.

Once the liquid limit, plastic limit, and shrinkage limit are determined, these values can be used to classify the soil based on its plasticity characteristics. Common classifications include the following:

- Non-plastic is when PL and LL are both very low.
- Low plasticity is when PL is low, and LL is moderate.
- High plasticity is when PL and LL are both relatively high.

The plasticity index (PI) is the difference between the liquid limit (LL) and the plastic limit (PL). PI of the whole sample (PI_{ws}) calculated by the PI and by the fraction of the soil that passes the 0.425 mm sieve ($P_{0.425}$) (Eq. 5) against the clay percentage of each sample (54).

$$PI_{WS} = \mathrm{PI} \times \left(\frac{P_{0.425}}{100} \right) \tag{5}$$

The results for each sample taken are plotted on an A-line graph showing soil consistency based on the Atterberg limits, and this method provides insights into how the soil's behaviour changes with moisture content to aid in classifying and assessing soil types.

4.3.4 Van der Merwe Method [41]

The Van der Merwe chart, also known as the Van der Merwe shrink-swell chart, is a graphical tool used to assess the potential expansiveness of particularly clayey soils [41]. It helps in determining whether a soil is susceptible to significant volume changes (swelling and shrinking) with changes in moisture content. The LL and PI values can be plotted on the Van der Merwe chart by plotting the LL on the *x*-axis, and the PI is on the *y*-axis. Each LL-PI combination results in a specific point on the chart, and the position of the point on the Van der Merwe chart provides a quick visual assessment of the soil's expansiveness as per the below zones which indicate a potential percentage volume change:

- Low (< 2%)
- Medium (2%)
- High (4%)
- Very high (8%)

4.3.5 Grading Modulus [44]

The grading modulus (*GM*) is the cumulative percentages retained on the 2 mm (P_2), 425 µm ($P_{0.425}$), and 75 µm ($P_{0.075}$) as shown in (Eq. 6) (parameters simplified to be in mm and consistent throughout this article). A minimum value of GM = 0 indicates a very fine soil with all particles finer than 0.075 mm, and a maximum value of GM = 3 indicates that all the soil is coarser than 2 mm.

$$GM = \frac{300 - (P_2 + P_{0.425} + P_{0.075})}{100} \tag{6}$$

4.3.6 Specific Gravity (SANS 5844–2)[45]

The specific gravity of the soil is dimensionless and represents the ratio of the density of the soil solids to the density of water. Different soils have different specific gravity values, and it is an important parameter for soil classification and engineering calculations, such as determining void ratios, porosity, and compaction characteristics.

A representative soil sample is collected and cleared of any organic material or foreign particles. The sample is then weighed and added to a glass jar with a known volume of water. The volumes of the water and soil are recorded. The soil is then removed, and the displacement of the water is measured. Specific gravity of the soil is calculated according to (Eq. 7).

$$\mathrm{SG} = \frac{M_1}{M_1 - V_W} \times \frac{V_W}{V_d} \tag{7}$$

where *SG* is the specific gravity of the soil (-/-), M_1 is the weight of the dry soil sample (kg), M_w is the weight of the container with water including the soil (kg), V_w is the volume of water (m^3), and V_d is the volume of water displaced by the soil sample (m^3).

4.4 MOD AASHTO Compaction Tests

All samples were submitted for MOD AASHTO compaction testing that was conducted according to the methodology set out in AASHTO T 180 [46]. The Modified Proctor Test is a standard laboratory test used to determine the maximum dry density and optimum moisture content of a soil or aggregate material for a given compaction effort. This test is commonly used in the construction of roads, foundations, and

other civil engineering projects to assess the suitability of materials. The American Association of State Highway and Transportation Officials (AASHTO) provides guidelines for conducting this test as follows:

- Sample preparation: Prepare the soil or aggregate sample by removing all organic material and air-drying.
- Determination of initial moisture content: Conducted as per §4.3.2.
- Test specimen preparation: The sample is divided into several portions of known mass and volume to calculate dry density and additional water is added to each portion in quantities ranging below and above anticipated OMC values.
- Compaction: Each sample is placed in a compaction mould in layers and is subjected to a specified number of blows from a standard compaction hammer or mechanical compactor as outlined in §2.5.
- Dry density and optimum moisture content calculation: The dry density for each compaction effort is calculated using the measured mass and mould volume. These are plotted on a curve of dry density versus moisture content and the point on the curve where the dry density is maximum is determined that represents the maximum dry density and the corresponding moisture content is the optimum moisture content.

5 Results

5.1 Soil Profiles

The general soil profile sequence encountered at the MSTF site from top to bottom is as follows:

- Cohesive residual gabbro: slightly moist, orange, brown to dark reddish brown, soft, fissured, sandy clay or gravelly clay with abundant coarse, medium, and fine, subangular to subrounded gravel and cobbles.
- Non-cohesive residual gabbro: light-yellow grey frequently blotched orange, loose becoming dense with depth, relict textured and structured, clayey sand with coarse, medium, and fine, subangular to subrounded gravel and cobbles of gabbro.

Fig. 23 Photographs of sampled soil horizons (© Jason Tunnell)

The general soil profile sequence encountered at the SMC site from top to bottom is as follows:

- Cohesive residual gabbro: moist, soft, intact silty clay and resembled the colour of its overlying surficial material which was generally a dark red colluvium.
- Non-cohesive residual gabbro: moist, dark yellowish grey speckled black, medium dense, intact, silty sand with occasional boulders and core stones of gabbro norite.

Figure 23 shows photographs of the material sampled for this investigation.

5.2 XRD Analyses

Table 5 and Fig. 23 show the relative abundance of all minerals found in the samples which show that predominant mineral found in both the MTSF and SMC non-cohesive samples is plagioclase at high average percentages of 47.57% and 61.84% respectively. This changes in the cohesive samples which are predominantly composed of clay minerals such as kaolinite and smectite, showing lower levels of plagioclase of 22.89% and 12.89%. The cohesive samples both contained between 29 and 47% kaolinite which was not present in the non-cohesive samples.

The plagioclase found in the non-cohesive samples most likely broke down into kaolinite whilst undergoing chemical weathering (decomposition). Other noticeable distinctions between the cohesive and non-cohesive samples are the decreased percentages of augite and enstatite in the cohesive samples, and the slightly higher amounts of smectite (10.88% and 17.94%) compared to their non-cohesive counterparts.

Plagioclase in the MTSF and SMC cohesive residual soils was 22.14% and 12.89% respectively, and in the non-cohesive residual soils, it was 47.57% and 61.84%, respectively. Kaolinite and smectite in the MTSF and SMC cohesive residual soils were 29.96% and 10.88%, and 40.16% and 17.94%, respectively (Fig. 24).

The plagioclase found in the non-cohesive samples most likely broke down into kaolinite whilst undergoing chemical weathering (decomposition). Other noticeable distinctions between the cohesive and non-cohesive samples are the decreased percentages of augite and enstatite in the cohesive samples and alternatively, the slightly higher amounts of smectite (10.88% and 17.94%) compared to their non-cohesive counterparts.

Plagioclase in the MTSF and SMC cohesive residual soils was 22.14% and 12.89% respectively, and in the non-cohesive residual soils, it was 47.57% and 61.84%, respectively. Kaolinite and smectite in the MTSF and SMC cohesive residual soils were 29.96% and 10.88%, and 40.16% and 17.94%, respectively.

Table 5 XRD results (relative abundance)

ID	Actinolite	Augite	Anatase	Chlorite	Enstatite	Hematite	Kaolinite	Lizardite	Orthoclase	Plagioclase	Quartz	Smectite	Talc	Total
Non-cohesive residual soil														
MTSF	-	7.04%	-	0.45%	28.72%	-	-	-	-	49.32%	4.73%	9.27%	0.47%	100.00%
	0.20%	6.21%	-	0.98%	28.56%	-	-	-	-	47.07%	5.23%	11.57%	0.18%	100.00%
	1.52%	8.28%	-	0.34%	29.88%	-	-	-	-	47.88%	5.62%	6.20%	0.28%	100.00%
	0.28%	6.50%	-	1.51%	27.86%	-	-	-	-	47.63%	5.74%	9.83%	0.65%	100.00%
	-	5.45%	-	1.06%	32.13%	-	-	-	-	45.97%	5.17%	10.19%	0.02%	99.99%
Average:	**0.67%**	**6.70%**	**-**	**0.87%**	**29.43%**	**-**	**-**	**-**	**-**	**47.57%**	**5.30%**	**9.41%**	**0.32%**	**100.00%**
SMC	1.92%	8.73%	-	-	8.43%	-	-	0.56%	-	58.15%	2.48%	9.01%	10.73%	100.01%
	1.66%	7.25%	-	-	9.67%	-	-	0.66%	-	58.47%	1.19%	10.58%	10.52%	100.00%
	0.74%	4.04%	-	-	8.61%	-	-	1.26%	-	64.67%	3.18%	10.77%	6.73%	100.00%
	0.88%	3.98%	-	-	7.34%	-	-	-	-	64.37%	3.59%	14.25%	5.58%	99.99%
	0.89%	7.56%	-	-	3.98%	0.07%	-	0.82%	-	63.53%	3.15%	11.35%	8.64%	99.99%
Average:	**1.22%**	**6.31%**	**-**	**-**	**7.61%**	**0.07%**	**-**	**0.83%**	**-**	**61.84%**	**2.72%**	**11.19%**	**8.44%**	**100.00%**
Cohesive residual soil														
MTSF	-	1.30%	-	-	20.58%	-	30.49%	-	8.38%	21.22%	7.79%	8.52%	1.73%	100.01%
	-	1.78%	-	-	19.84%	-	30.58%	-	5.11%	20.84%	8.78%	11.67%	1.40%	100.00%
	-	1.05%	-	-	19.74%	-	28.82%	-	6.47%	23.24%	7.19%	11.47%	2.01%	99.99%
	-	0.98%	-	-	17.94%	-	30.80%	-	7.03%	21.46%	7.00%	11.04%	3.75%	100.00%
	-	2.20%	-	-	17.68%	-	29.10%	-	5.26%	23.96%	8.05%	11.70%	2.05%	100.00%
Average:	**-**	**1.46%**	**-**	**-**	**19.16%**	**-**	**29.96%**	**-**	**6.45%**	**22.14%**	**7.76%**	**10.88%**	**2.19%**	**100.00%**
SMC	5.69%	0.37%	0.26%	-	11.00%	0.31%	32.79%	-	-	15.28%	2.15%	15.06%	17.09%	100.00%
	7.24%	0.45%	0.35%	-	7.46%	0.23%	47.80%	-	-	11.16%	1.74%	16.58%	6.99%	100.00%
	8.80%	0.58%	0.56%	-	8.84%	0.23%	41.46%	-	-	11.38%	1.66%	15.16%	11.33%	100.00%
	5.21%	0.61%	0.45%	-	4.09%	0.36%	41.43%	-	-	14.72%	2.80%	19.57%	10.75%	99.99%
	3.92%	0.47%	0.52%	-	4.35%	0.52%	37.30%	-	-	11.89%	5.07%	23.35%	12.59%	99.98%
Average:	**6.17%**	**0.50%**	**0.43%**	**-**	**7.15%**	**0.33%**	**40.16%**	**-**	**-**	**12.89%**	**2.68%**	**17.94%**	**11.75%**	**99.99%**

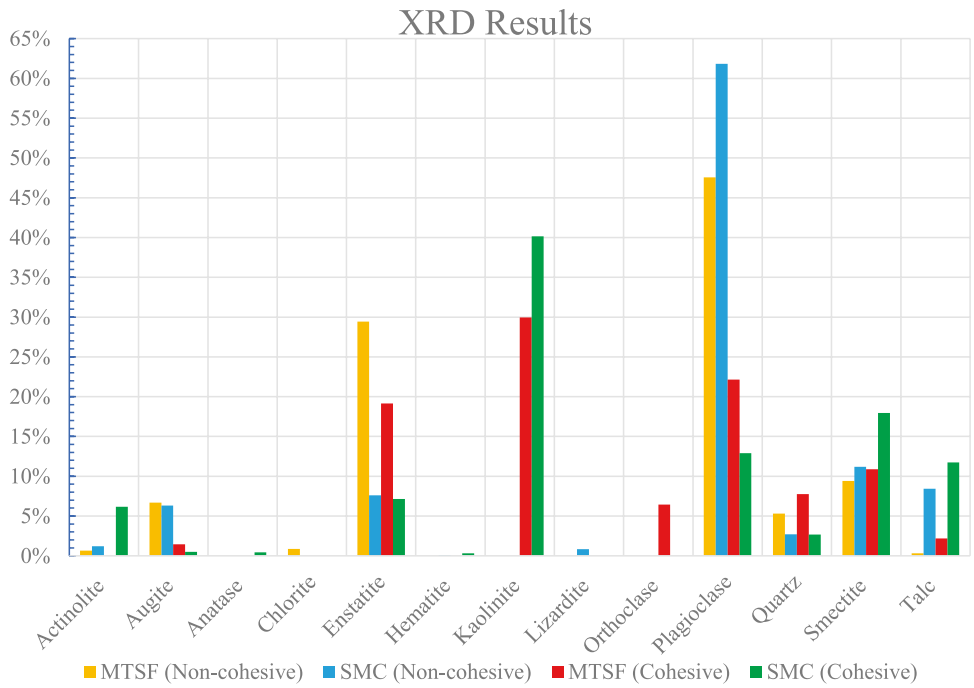

Fig. 24 XRD results per mineral and site

Table 6 Foundation indicator test results

Site	USCS	Grading analysis				Atterberg limits				Moisture content (%)	GM	SG
		Gravel %	Sand %	Silt %	Clay %	Liquid Limit	Linear Shrinkage	Plastic Limit	Plasticity Index			
Cohesive residual soil												
MTSF	SC	7	50	16	27	55.0	24.5	22.0	33.0	23.1	0.77	2.77
	CH	3	39	14	44	69.0	29.0	31.0	38.0	38.5	0.46	2.71
	CH	9	44	19	28	62.0	27.0	27.0	35.0	25.1	0.74	2.77
	CH	1	42	14	43	71.0	29.5	28.0	43.0	8.8	0.46	2.76
	CH	1	42	13	44	69.0	30.5	27.0	42.0	42.2	0.52	2.74
Average(n=5)		**4**	**43**	**15**	**37**	**65.2**	**28.1**	**27.0**	**38.2**	**27.5**	**0.59**	**2.75**
SMC	CH	3	23	19	55	73.0	25.5	36.0	37.0	-	0.30	2.76
	CH	1	12	24	63	61.0	22.0	28.0	33.0	-	0.14	2.61
	CH	0	19	27	54	60.0	14.0	30.0	30.0	-	0.15	2.73
	CH	20	25	18	37	54.0	13.5	26.0	28.0	-	0.89	2.69
Average(n=4)		**6**	**20**	**22**	**52**	**62.0**	**18.8**	**30.0**	**32.0**	**-**	**0.37**	**2.70**
Non cohesive residual soil												
MTSF	SW-SM	18	77	4	1	-	0.5	-	SP	10.0	1.82	2.96
	SW-SM	56	41	2	1	-	0.5	-	SP	10.8	2.34	2.89
	GP-GC	63	34	2	1	32.0	6.5	19.0	13.0	12.4	2.41	2.81
	GP-GC	61	35	3	1	27.0	4.5	18.0	9.0	11.0	2.31	2.87
	SW-SC	58	38	3	1	29.0	5.0	19.0	10.0	8.0	2.31	2.83
	SW	55	43	1	1	-	0.5	-	SP	5.7	2.34	2.91
	SC	29	63	6	2	29.0	6.5	17.0	12.0	21.2	1.73	2.83
Average(n=7)		**49**	**47**	**3**	**1**	**29.3**	**3.4**	**18.3**	**11.0**	**11.3**	**2**	**3**
SMC	SC	8	73	15	4	32.0	6.0	21.0	11.0	-	1.24	2.67
	SC-SM	10	77	11	2	28.0	3.0	23.0	5.0	-	1.31	2.74
	SC	0	68	22	10	33.0	7.0	19.0	14.0	-	0.82	2.76
	SM	4	79	13	4	-	0.5	-	SP	-	1.23	2.84
	SW-SM	19	73	7	1	-	0.5	-	SP	-	1.72	2.87
Average(n=5)		**8**	**74**	**14**	**4**	**31.0**	**3.4**	**21.0**	**10.0**	**-**	**1.26**	**2.78**

5.3 Foundation Indicators

The Atterberg limits and grading analysis are presented in Table 6 and the particle size distribution curves in Fig. 25

. The Unified Soil Classification System (USCS) is used to classify soils in terms of the amount of clay (C), silt (M), sand (S), gravel (G), and organic (O) materials, whether plasticity is low (L) or high (H), and whether the soil is

poorly graded (P) or well-graded (W). This is indicated in with two capital letters of which the first is dominant [47].

Cohesive residual soil samples taken from the MTSF site classify as clay of high plasticity in the USCS (CH) with one sample classifying as clayey sand (SC). An average clay content of 37% was returned for the MTSF cohesive samples with the higher clay percentage returned for these samples being supported by a low grading modulus (GM < 1). The average plasticity index (PI) of material is 38.2 (ranging between 33 and 43). The particle size distribution (Fig. 25) for this material correlates to the results and is indicative of a soil with a high clay content.

The SMC cohesive samples generally classify as clays of high plasticity (CH) because the samples have a high average clay content of 52% which correlates to the low average GM of 0.37 and an average plasticity index of 32.

Non-cohesive samples taken from the MTSF site returned a high average gravel and sand percentage of 49% and 47% respectively, and these results are supported by the high GM of 2. The samples generally had a very low clay percentage (1%), and this is supported by the low plasticity index of 11% as shown in Fig. 25. In terms of USCS, the samples ranged from well graded silty sand (SW-SM) to poorly graded clayey gravel (GP-GC).

The non-cohesive samples taken from the SMC site classify as a mixture of clayey sand (SC) and silty sand (SM). The samples had a lower gravel content than the MTSF samples and this is supported by the lower GM of 1.26. The samples did however return a high sand fraction of 74% and a low plasticity index of 10 (ranging from slightly plastic to 11).

The calculated GM values are in line with what is expected and confirm the categorisation of the samples into cohesive and non-cohesive soils with the cohesive soils having GM values in the range of 0.14–0.89, and the non-cohesive soils having GM values in the range of 0.82–2.41.

It is evident from the graphical representation of the PSD for the samples taken that the samples identified as cohesive have more fines (clay and silt) than their non-cohesive counter parts. In general, both the cohesive and non-cohesive samples taken from the SMC site contained more fines than the MTSF samples. The MTSF non-cohesive samples contained considerably more gravel sized particles than any of the other samples taken from the two sites. The higher clay fractions shown in the particle size distribution graphs for the cohesive samples are concurrent with the XRD results which showed higher clay mineral contents for the cohesive samples.

5.4 Atterberg Limits

The Atterberg limits for the fine-grained fractions of the samples were plotted on a plasticity graph (A-line) using the relationship between the plasticity index (PI) and liquid limit (LL) and are depicted in Fig. 26.

From Fig. 26, all the non-cohesive samples are shown to have a low plasticity, and all the cohesive samples had a high to very high plasticity. Most of the cohesive samples plotted above the A-line indicating that the fines component of the samples is predominantly clay with exception to one cohesive sample from the SMC site.

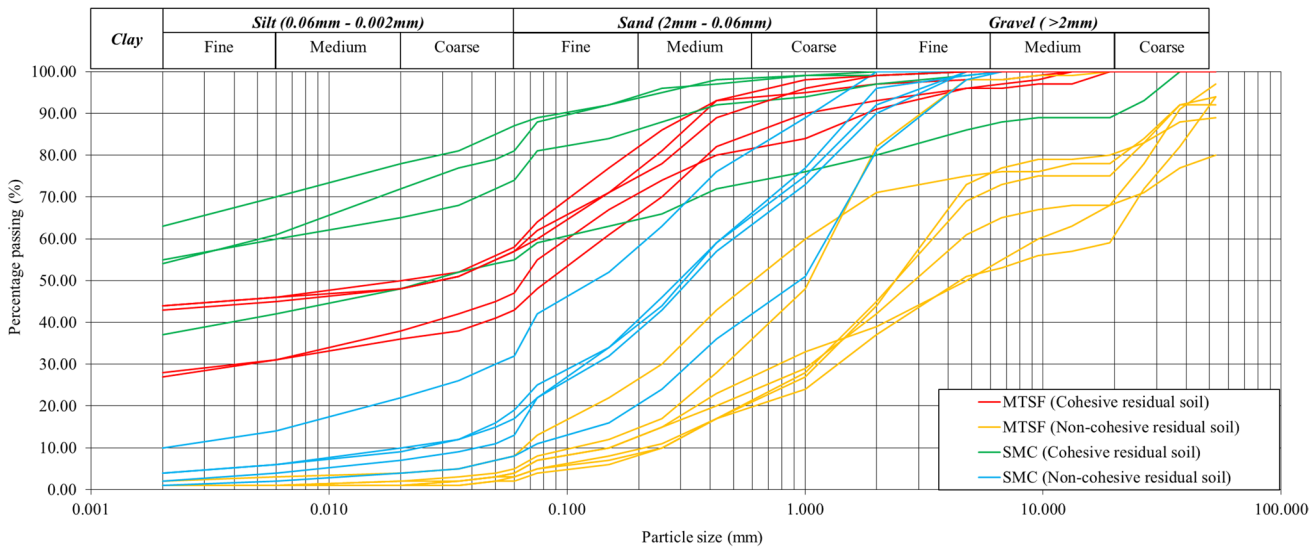

Fig. 25 Particle size distribution graph of all samples

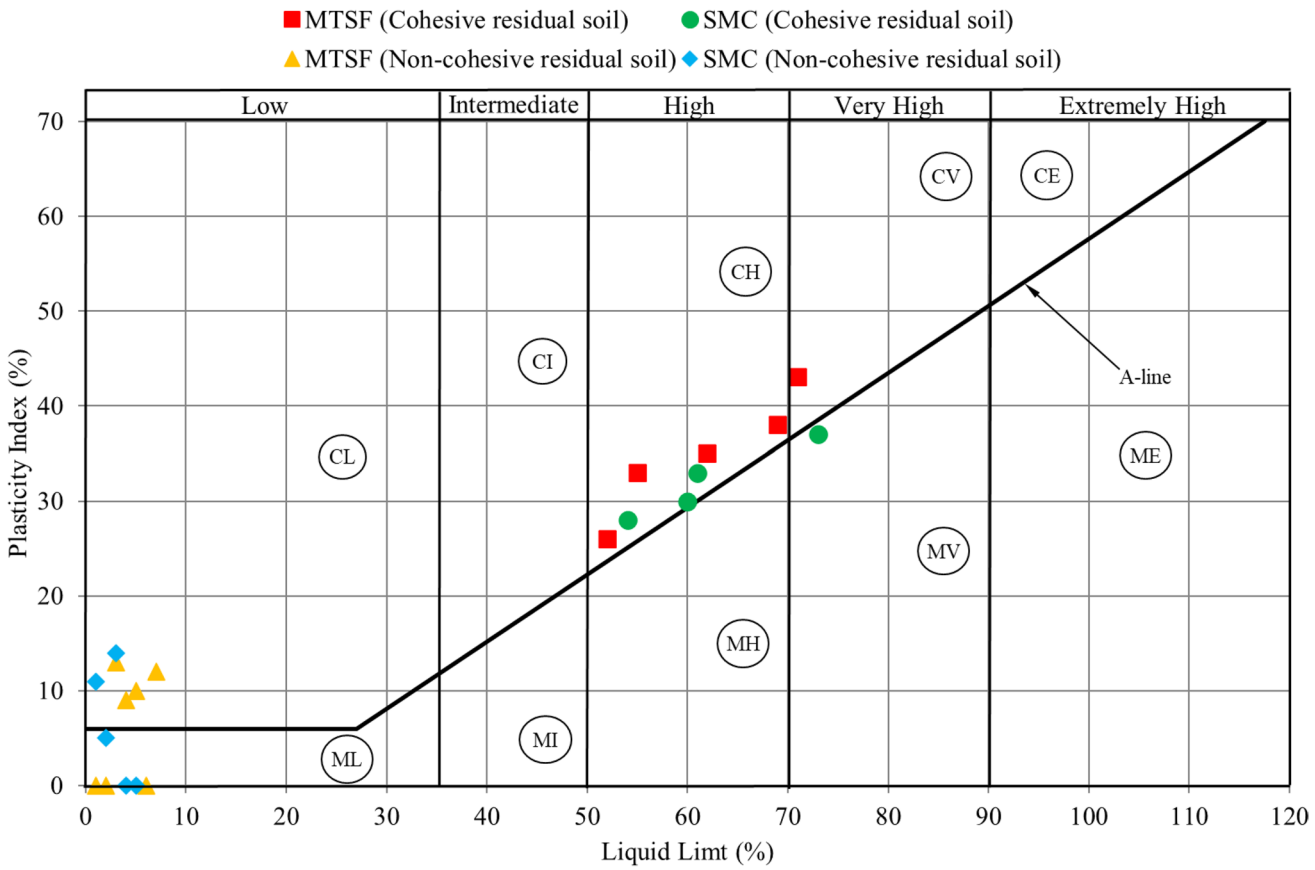

Fig. 26 Samples indicated on the Atterberg limit graph

5.5 Potential Expansiveness

The results of the foundation indicator tests were plotted on the Van der Merwe chart (Fig. 27) to assess the potential expansiveness of the soil samples.

According to the Van der Merwe potential expansiveness graph, it is evident that all the non-cohesive material tested is generally characterised by a low potential expansiveness (< 2%). With the exception of one MTSF cohesive sample plotting in the low range (< 2%), all the cohesive samples tested plotted in the high to very high range (4–8%). This is indicative of high activity which indicates possible instability.

5.6 MOD AASHTO Compaction Testing

The MDD and the OMC relationship were determined for 23 samples. A summary of the moisture and density relationship of the samples is included in Table 7. (Eq. 8) shows the relationship between a soil's dry density and its specific gravity assuming that the specific gravity of the sample remains constant at a given moisture content.

$$\rho_d = \frac{\rho_w}{\left(\frac{w}{100} + \frac{1}{SG}\right)} \tag{8}$$

where ρ_d is the dry density (kg/m^3), ρ_w is the density of water (1000 kg/m^3), w is the water content (%), and SG is the specific gravity (unitless).

The cohesive samples returned a lower MDD and a higher OMC in general compared to the non-cohesive samples. The cohesive residual samples taken from the MTSF site returned an average MDD of 1 907 kg/m^3 at an average OMC of 14.5% whilst the SMC cohesive residual samples returned an average MDD of 1 667 kg/m^3 at an average OMC of 17.6%. The non-cohesive samples taken from the MTSF and SMC sites both returned high average MDD results of 2 066 kg/m^3 and 2 068 kg/m^3, respectively. The OMC was also found to be lower than that of the cohesive samples at 10.4% and 10.8%.

For quality control purposes, the moisture-density relationship of the samples was compared to the 0%, 5%, and 10% air void curves shown in Fig. 28 for a specific gravity (SG) deemed applicable to the material types. The 0% air void curve represents the maximum possible

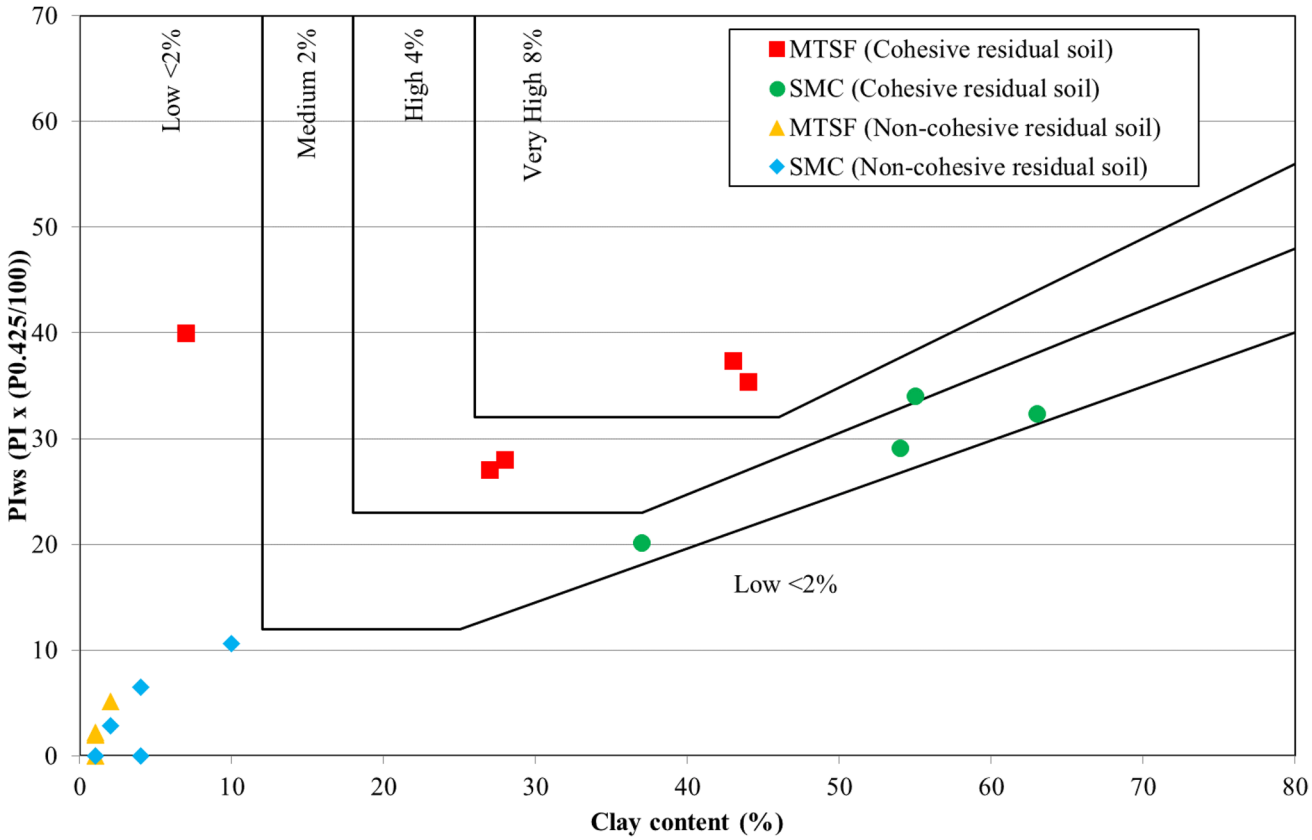

Fig. 27 Van der Merwe potential expansiveness graph [41]

Table 7 MOD AASHTO results

Site	MDD (Kg/m³)	OMC (%)	SG	Site	MDD (Kg/m³)	OMC (%)	SG
Cohesive residual				**Non-cohesive residual**			
MTSF	1 827	15.3	2.77	**MTSF**	2 099	9.1	2.96
	1 943	14.7	2.71		2 136	10.4	2.89
	1 938	13.1	2.77		2 055	10.4	2.81
	1 921	14.3	2.76		2 108	9.5	2.87
	1 957	13.8	2.74		2 088	10.9	2.83
	1 857	15.7	2.72		1 930	13.0	2.83
Average(n=6):	**1 907**	**14.5**	**2.74**	**Average(n=6):**	**2 069**	**10.6**	**2.86**
SMC	1 611	15.6	2.76	**SMC**	2 096	10.3	2.67
	1 620	20.0	2.61		2 085	10.5	2.74
	1 625	14.5	2.73		2 079	10.9	2.76
	1 649	18.4	2.69		2 097	10.3	2.84
	1 708	19.7	-		2 037	11.7	2.87
	1 789	17.1	-		2 016	11.3	2.00
Average(n=6):	**1 667**	**17.6**	**2.70**	**Average(n=6):**	**2 068**	**10.8**	**2.65**

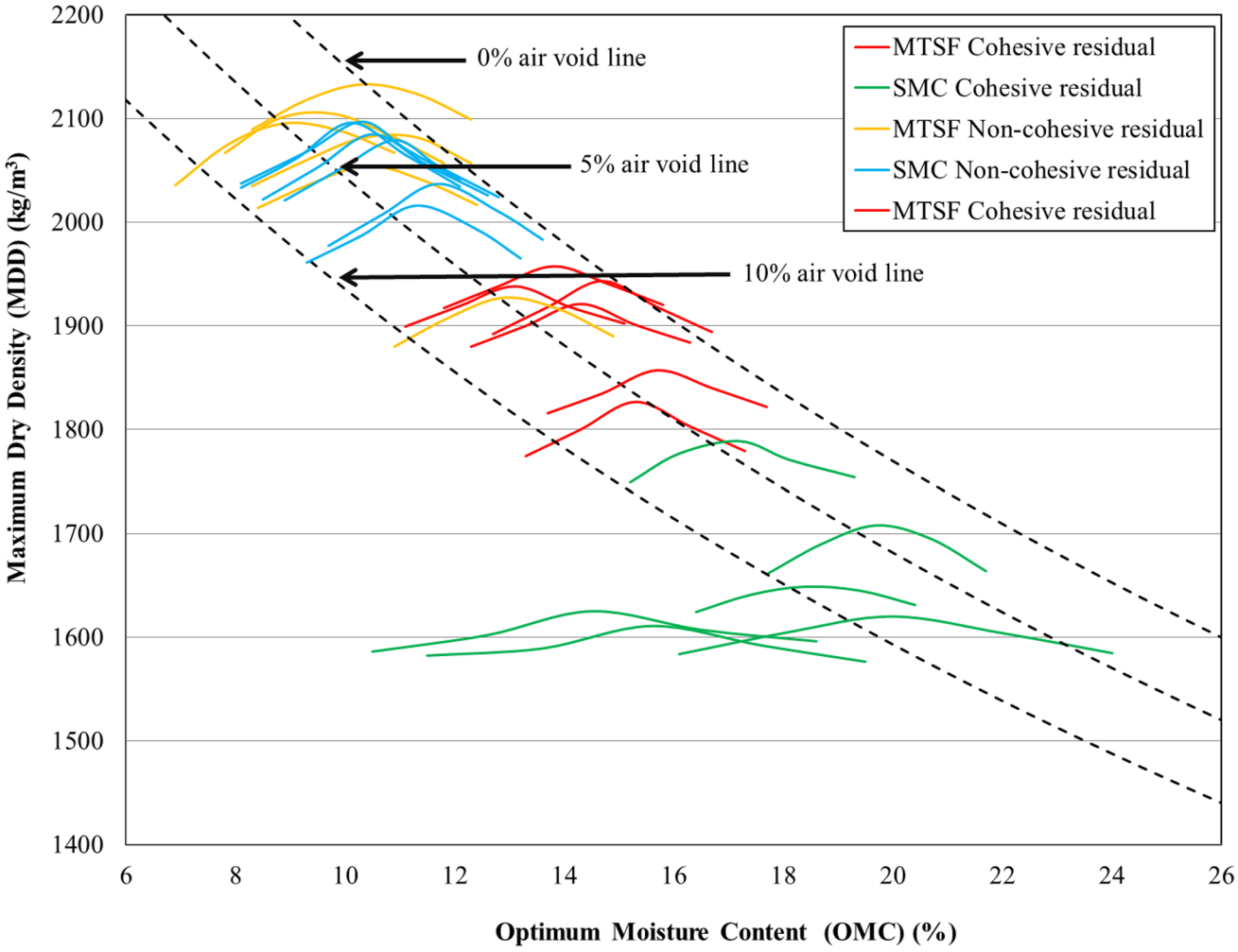

Fig. 28 MOD AASHTO curves

density that the soil can be compacted to for a given water content. This degree of compaction is however unattainable in practice and serves as a quality control check to judge the correctness of the laboratory data as reported compaction results should plot completely to the left of the 0% air void curve. Additionally, if reported compaction results plot left of the 10% air void line, it can be assumed that the result does not necessarily represent the maximum density of that sample.

From Fig. 28, it is evident that the majority of the samples plot between the 0 and 5% air void lines with the exception to some of the SMC cohesive samples. The position of the air void lines was calculated using an average specific gravity of 2.74 for all the MOD samples taken. It is evident from the results that in general the non-cohesive samples tend to return a higher MDD at a lower OMC than the cohesive samples.

6 Discussion

Based on the literature, a variety of governing elements must be considered when determining a soil's compaction characteristics. Factors on compaction such as compactive effort and compaction method (machinery used) are defined by the project specifications, and it can be altered based on better understanding of the soils used for construction. Increased applied compactive efforts cause an increase in compaction, and the compaction method will affect the ease and speed of compaction.

It is important to use the correct machinery based on the properties of the geological media being compacted. If the machinery is too light, then proper compaction will not be achieved, and if the machinery is too heavy, the soil's physical properties can be altered due to breaking of mineral grains. These external factors are not relevant for this

investigation as it was mitigated by applying the same compaction effort (MOD AASHTOO) to all samples.

The variable results are the outcome of factors such as particle size and moisture content. It is evident that samples that exhibited smaller particle sizes and greater moisture contents produced lower maximum dry densities and therefore lower levels of compaction at the same compaction effort.

All the samples tested from the two sites presented had similar mineralogy comprising predominately plagioclase in the non-cohesive samples and kaolinite in the cohesive samples, and the major difference identified between the sample sets was the presence of higher amounts of clay minerals (kaolinite, smectite) and talc in the cohesive samples. The relative abundance of other minerals such as augite and enstatite was found to be lower in the cohesive samples whilst the remaining mineral constituents did not vary much between the different sample sets. Figure 29 presents a graphical illustration of the average mineral abundance between the non-cohesive (outer ring) and cohesive (inner ring) samples found at the two project sites.

The grading of the residual soils is dependent on the parent rock mineralogical composition, and then on the chemical weathering (decomposition) and/or physical (mechanical) weathering disintegration processes due to weathering of the rocks. Chemical weathering decomposes rock to change mineralogy and structure, and physical weathering disintegrates rock into finer fragments of the same minerals. These can coexist, but the prior dominates in humid environments, and the latter in arid environments.

The cohesive samples from both sites overlie the non-cohesive horizons and have therefore been more exposed to the elements including oxygen and water increasing the influence of chemical weathering. This caused the cohesive samples forming due to being highly reworked, and therefore losing the inherent parent structure, and increasing the amount of silt and clay size secondary minerals present. This causes the changes to the material's grading and chemical (mineralogical) composition.

The grading of the MTSF samples is mostly coarser than the SMC samples. Soils that had a coarser grain size and plotted higher on the PSD graphs generally produced a higher maximum dry density than the soils with finer gradings. Figure 30 provides a graphical representation of the varying gradings of material found across the four sites.

Alcott showed the best correlation between compaction characteristics and the soil grading was found to exist for the clay fraction of a soil [30]. Figure 31 shows the MDD obtained at the optimal OMC correlated with the clay and gravel contents of the samples. When comparing these compaction characteristics to the average gravel percentages, a low correlation was found (0.2685–0.3722 or about 27–37%), and the average clay percentages produced a high correlation (0.9134–0.9829 or about 91–98%).

All the cohesive samples tested returned higher Atterberg limits than the non-cohesive samples due to the increased

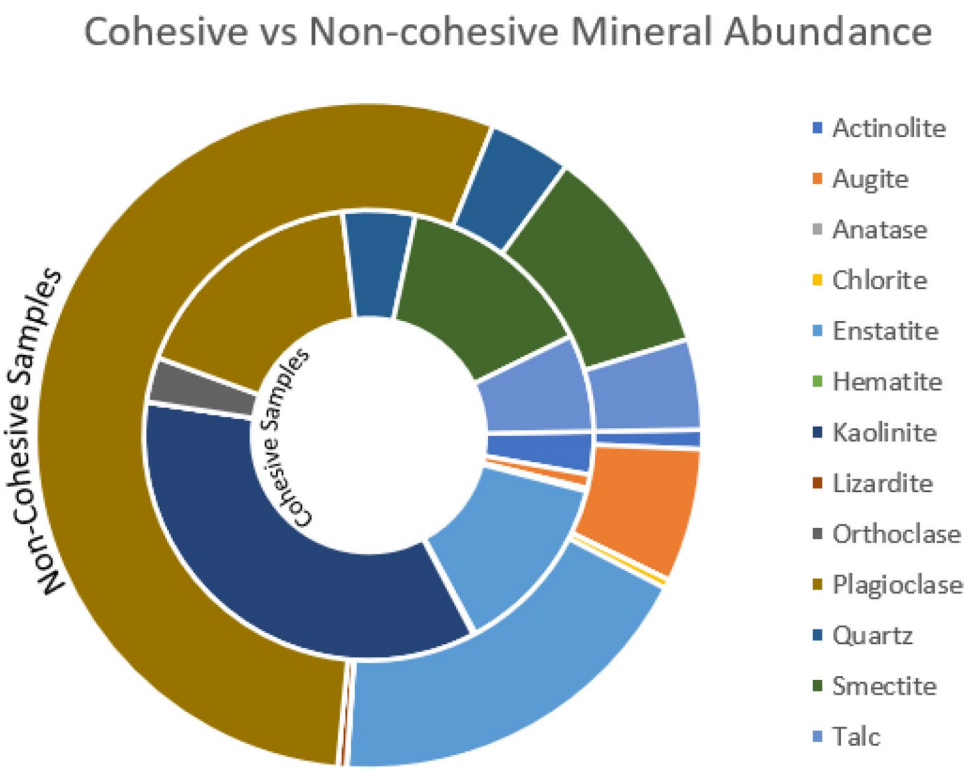

Fig. 29 Mineral abundances of cohesive vs non-cohesive samples

Fig. 30 PSD of four sites

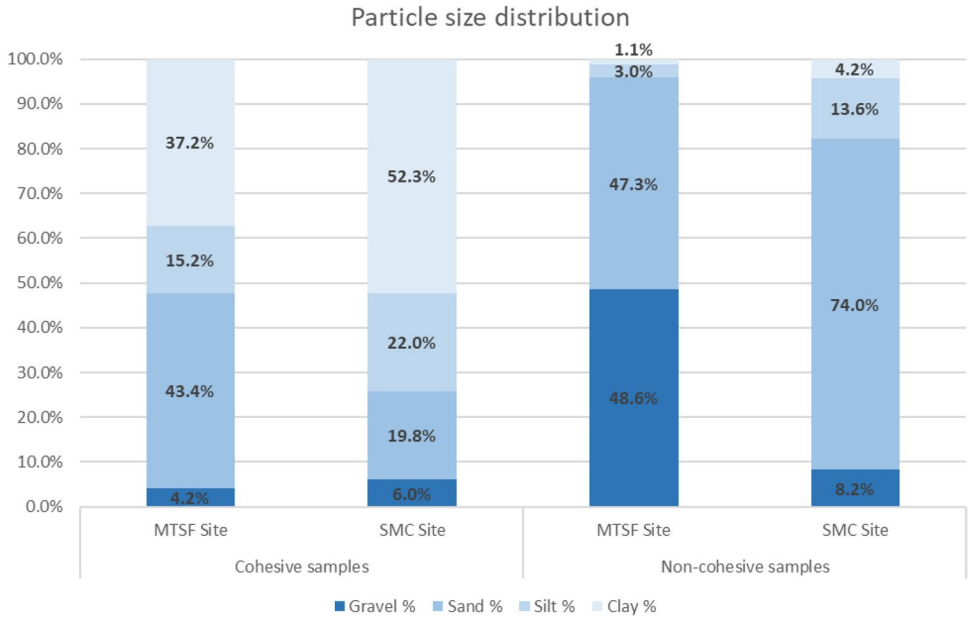

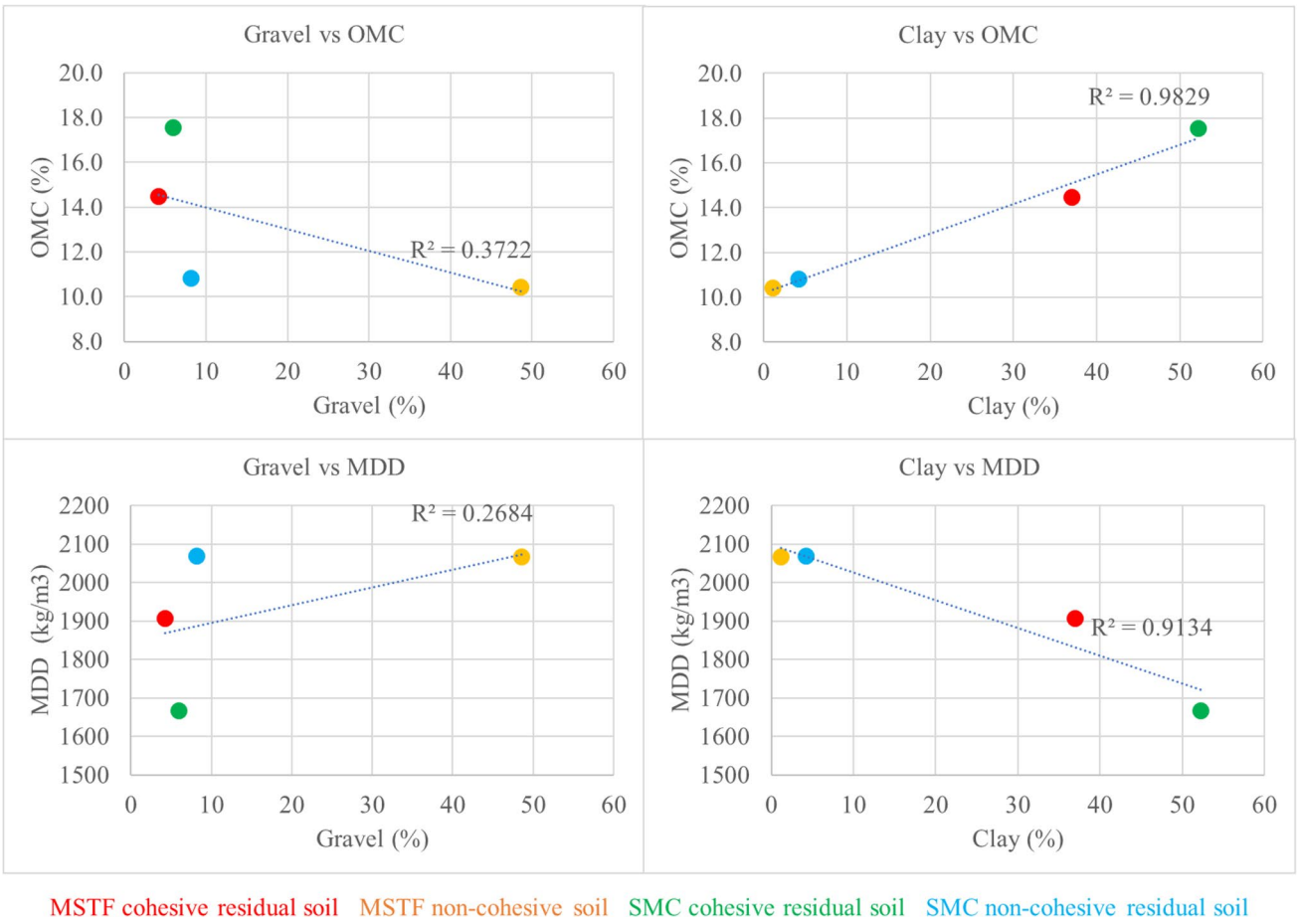

Fig. 31 Gravel and clay percentages compared to compaction characteristics including optimal moisture content and maximum dry density

Table 8 Atterberg limits vs. compaction

Sample set	A-line result	VDM result	Compaction result	
			MDD (Kg/m³)	OMC (%)
MTSF (Cohesive soil)	high to very high activity	medium to high expansiveness	1 907	14.5
MTSF (Non-cohesive soil)	Low activity	low expansiveness	2 066	10.4
SMC (Cohesive soil)	high to very high activity	medium to high expansiveness	1 667	17.6
SMC (Non-cohesive soil)	Low activity	low expansiveness	2 068	10.8

relative abundances of fine fraction silt and clay minerals. The cohesive samples taken from the SMC site in Zimbabwe had the highest clay contents, and due to that higher Atterberg limits. This correlates to the climatic conditions for the site that has increased rainfall and therefore more chemical weathering resulting in the formation of secondary minerals that are clayey in nature such as kaolinite and smectite. A summary of these results is presented in Table 8.

Soils with a higher clay content have a higher affinity to retain water and therefore a higher OMC. As a clayey soil approaches OMC, compaction becomes difficult due to the higher pore pressures which counter the effects of compaction. This is evident in the results presented as samples containing more clay minerals plotted higher on the A-line and VDM graphs (Fig. 25 and Fig. 26).

The cohesive samples returned lower levels of compaction than their non-cohesive counterparts. The smaller particle sizes in these samples mean that a greater surface area is available for the water particles to adhere to, causing higher pore pressures and subsequently a lower maximum dry density. Additional to the already lower maximum dry density exhibited by clay particles increased activity and expansiveness will result in an overall decrease in compaction over time. Although the large vertical stresses associated with a TSF will have a large bulb of influence and most likely affect the soils underlying the prepared foundation, ensuring proper compaction of the foundation will have an effect on increasing stability and reducing near-surface shearing.

7 Conclusions

The mineralogy of a soil determines its physical and chemical properties and they both directly and indirectly affect a soil's compaction characteristics such as water content and particle size distribution. The compaction of the underlying strata of a tailings storage facility will greatly affect its stability by mitigating settlement, shearing and ultimately result in a stable, safer foundation.

7.1 Main Findings

This study aimed to investigate residual gabbro soil through compiling appropriate mineralogical, mechanical, and geotechnical data to determine its effect on compaction during the construction of the foundations of tailings storage facilities. Residual gabbro soils were split into non-cohesive and cohesive sample sets for the Great Dyke in Zimbabwe and the Bushveld Igneous Complex in South Africa. Both regions are known for their platinum-rich soils but pose very different climatic conditions which in turn provided insight into different levels of chemical weathering.

The collected samples were tested for compaction characteristics and mineralogy. From literature and the results presented, it is evident that mineralogy plays an important role in determining the compaction characteristics of soil. The major findings of interest in this study are as follows:

- Residual gabbro soils that are exposed to the elements such as high rainfall and temperatures tend to be more cohesive by nature due to greater levels of chemical weathering and results in the formation of more clayey and silty secondary minerals.
- The presence of more cohesive material such as silt and more importantly clay in a soil tends to increase the optimal moisture content due to clay's ability to physically and chemically *hold* water molecules more tightly than sands or silts. There is a strong correlation between a soil clay content and its compaction characteristics. From the results presented, a soil clay content is directly proportional to its optimal moisture content and inversely proportional to its maximum dry density. 2:1 layered silicate clay such as smectite encountered on the SMC site in Zimbabwe exhibits greater levels of activity and expansiveness due to their ability to absorb more water and free exchangeable cations which further counters the effect of compaction.

These internal factors are largely controlled by the mineralogy of the soil and the chemical and physical properties of the samples being tested. The presence of clay minerals, specifically 2:1 layered silicates such as smectite, greatly decreases the compaction of a soil and increases the potential of shear failure due to high levels of water retention. This phenomenon is most likely due to increased pore pressures and swelling caused by the clay minerals which counteracts the effects of compaction and will further serve to decrease the stability of any foundation constructed using this material.

7.2 Limitations and Assumptions

Restrictions and limitations on the transportation of mineral samples out of Zimbabwe resulted in multiple accredited laboratories having to be utilised for this study. As noted in §5.6, some of the SMC cohesive samples plotted outside of the computed air void control lines bringing into question some of the results obtained. The authors are however of the opinion that sufficient testing was conducted and enough research from previous studies was utilised to justify the interpreted conclusions presented.

7.3 Way Forward

To assess the stability of foundations for tailings storage facilities and better understand the role mineralogy plays, further research into how mechanical compaction affects mineralogical fabric and texture should be conducted. Soil is a dynamic and ever-changing system, and the physical breakdown of minerals due to compaction can alter a soil's chemical and physical properties and therefore its stability. This specifically relates to its mineralogy that can change during wetting and oxidation, and its pores and structures that can be reduced or destroyed during compaction.

Ongoing research should utilise controlled mixes of soils in a laboratory setting by mixing soils of equal mineralogy that is the key driver of a soil's compaction capability. Varying amounts of dominant clay minerals such as kaolinite and smectite should be added to a standard sample in differing percentages to identify their effect on compaction and to correlate the results to the findings of this study. A better understanding of the mineralogical composition of the underlying geological units will assist during the design and operation of tailings dams across the world, ultimately aiding the management of these super structures as per the requirements set out in the new GISTM standards.

We now understand this, and research can build towards enhancing the knowledge of foundation design for tailings dams around the world to improve stability and ultimately decrease or prevent failures in the future.

Acknowledgements I wish to express my appreciation to the following organisations and persons who made this project report possible:

• I would like to express my sincere gratitude to my supervisor, Prof Matthys Dippenaar, for his continuous guidance, support, motivation, and knowledge throughout this project.

• Mr Gerrie Janse van Rensburg, for all his assistance and laboratory work done at Specialised Testing Laboratory.

• Ms Wiebke Grote for all her assistance and service from the Stoneman Laboratory, University of Pretoria.

• All my friends and colleagues, for there guidance and support throughout this project.

• My parents, Desre Guerini and Max Guerini, for always believing in me and pushing me to achieve my goals.

I would like to thank the following institutions and people:

• SRK Consulting, for allowing me to use project data and the financial support and guidance provided.

• The University of Pretoria for the financial, technical, and academic support provided.

• Mr Dipeen Dama and Brian Viriri of Anglo American and Zimplats respectively, for approving the use of laboratory results and the work conducted at the Mareesburg tailings dam and SMC tailings dam.

Author Contribution Jason Tunnell did the field work and interpreted all the data amounting to 75% of the work. Matthys Dippenaar supervised Jason Tunnell's work, assisted with the compilation of this paper, and reviewed and provided input into this paper amounting to 25% of the work.

Funding Open access funding provided by University of Pretoria.

Declarations

Competing Interests The authors declare no competing interests.

Open Access This article is licensed under a Creative Commons Attribution 4.0 International License, which permits use, sharing, adaptation, distribution and reproduction in any medium or format, as long as you give appropriate credit to the original author(s) and the source, provide a link to the Creative Commons licence, and indicate if changes were made. The images or other third party material in this article are included in the article's Creative Commons licence, unless indicated otherwise in a credit line to the material. If material is not included in the article's Creative Commons licence and your intended use is not permitted by statutory regulation or exceeds the permitted use, you will need to obtain permission directly from the copyright holder. To view a copy of this licence, visit http://creativecommons.org/licenses/by/4.0/.

References

1. Araya N, Kraslawski A, Cisternas LA (2020) Towards mine tailings valorization: recovery of critical materials from Chilean mine tailings. J Cleaner Prod 263:121555
2. Piciullo L, Storrósten EB, Zhonqiang L, Farrokh N, Lacasse S (2022) A new look at the statistics of tailings dam failures. Eng Geol 303(2):106657
3. Sousa, G. (2017) The top platinum producing countries in the world, WorldAtlas. Available at: https://www.worldatlas.com/articles/the-top-platinum-producing-countries-in-the-world.html (Accessed: 26 May 2024)
4. Zongjie L, Junrui C, Zengguang X, Tuan Q (2019) A comprehensive review on reasons for tailings dam failures based on case history. Adv Civ Eng 2019(9):1–18

5. ICMM (International Council on Mining and Metals). 2022. Global tailings review. Online at: https://globaltailingsreview.org/global-industry-standard/
6. Warburton, M., Hart, S. Ledur J., Scheyder E., Levine, A.J. 2020. Accessed 27 October /2022. The looming risk of tailings dams. Reuters. https://graphics.reuters.com/MINING-TAILINGS1/0100B4S72K1/index.html
7. Lumbroso D, Roca M, Petkovšek G, Davison M, Li HR, Goff C (2020) DAMSAT an eye in the sky for monitoring tailings dams. Int J Mine Water 40(4):113
8. Ghosh R (2012) Effect of soil moisture in the analysis of undrained shear strength of compacted clayey soil. Department of Construction Engineering, Jadavpur University, Kolkata, India, Kolkata
9. Nawaz M, Bourrie G, Trolard F (2013) Soil compaction impact modelling. A Rev Agron Sustain Dev 33:291–309
10. Namdar, A. 2011. Soil minerology and compaction techniques for improving foundations stability. Annals of Faculty Engineering Hunedoara – International Journal of Engineering. Tome IX. Fascicule 2. 4 233–238
11. Croney D, Croney P (1997) Design and performance of road pavements, 3rd ed. Proctor 1933
12. Proctor R (1933) Fundamental principles of soil compaction. Engineering News Record 111(9)
13. Kalantari, Behzad. (2012). Foundations on expansive soils: a review. Research Journal of Applied Sciences, Engineering and Technology. 4
14. CementConcrete.org. 2019. California bearing ratio (CBR test) of subgrade soil -procedure, apparatus, and use for pavement design. URL: https://cementconcrete.org/geotechnical/california-bearing-ratio-cbr-test/1914/ASTM D698
15. Patel A (2019) Geotechnical investigations and improvement of ground conditions. Woodhead Publishing. Elsevier Inc. https://doi.org/10.1016/C2018-0-01307-9
16. ASTM (Last update 2023) Standard test methods for in-place density and water content of soil and soil-aggregate by nuclear methods (shallow depth). Document No. D6938–17ae1
17. SANS 3001 GR35 - Civil engineering test methods Part GR35: determination of in-place dry density (sand replacement). South African Bureau of Standards
18. South Africa National Road Agency (2013) South African Pavement Engineering Manual, 1st ed
19. Harris WL (1971) The soil compaction process. In: Compaction of agricultural soils. American Society Agriculture Engineering, pp 9–44
20. Utest. 2022. Accessed 24 September 2022. RoadReader nuclear density gauges. URL: https:// www.utest.com.tr/en/23174/RoadReader-Nuclear-Density-Gauges
21. Das BM, Sobham K (2014) Principles of geotechnical engineering, 8th edn. Cengage learning, Florida
22. The Constructor. © date 2021. Factors affecting compaction of soils and their effect on different soils. https://theconstructor.org/geotechnical/factors-affecting-compaction-of-soils/5311/
23. Suryakanta. 2023. Factors affecting field compaction of soil. Built with GeneratePress. https://civilblog.org/2014/02/04/5-factors-which-affect-field-compaction-degree-of-compaction/
24. Di Sante M, Fratalocchi E, Mazzieri F (2016) Effects of variation in compaction water content on geotechnical properties of lime treated clayey soil. Procedia Engineering 158:63–68
25. Dejong-Hughes J, Moncrief JF, Voorhees WB, Swan JB. 2001. Soil compaction: causes, effects and control. LIBRARIES digital conservancy. St. Paul MN: University of Minnesota Extension Service. Retrieved from the University of Minnesota Digital Conservancy. https://hdl.handle.net/11299/55483
26. Rousseva S, Kercheva M, Shishkov T, Nikolaidis NP, Moraetis D, Krám P, Bernasconi SM, Blum WEH, Menon M (2017) Soil water characteristics of European SoilTrEC critical zone observatories. Adv Agron 142:29–72
27. Al-Atroush ME, Shabbir O, Almeshari B, Waly M, Sebaey TA (2021) A novel application of the hydrophobic polyurethane foam: expansive soil stabilization. Polymers 13:1335–1353. https://doi.org/10.3390/polym13081335
28. Kumari N, & Mohan C. 2021. Basics of clay minerals and their characteristic properties. In: G. M. D. Nascimento (ed.) Clay and clay minerals. Barnes & Noble. 224 pp
29. Chen M, Wu G-J, Gan B, Jiang W-H, Zhou J-W (2018) Physical and compaction properties of granular materials with artificial grading behind the particle size distributions. Adv Mater Sci Eng 2018:1–20
30. Alcott AD. 1970. Clay mineralogy and compaction characteristics of residual clay soils used in earth dam construction in the Ozark Province of Missouri". MSc dissertation. URL: https://scholarsmine.mst.edu/masters_theses/7177
31. Mungazi AA, Gwenzi W (2019) Cross-layer leaching of coal fly ash and mine tailings to control acid generation from mines. Mine Water Environ 38:613–616. https://doi.org/10.1007/s10230-019-00618-0
32. Mile M, & Mitkova. T. 2012. Soil moisture retention changes in terms of mineralogical composition of clays phase. Clay minerals in nature – their characterization modification and application. 328 pp
33. Web & Media. 2022. Accessed 6 September 2022. Weather and climate info. URL: https://www.besttimetovisit.co.za/south-africa/lydenburg-3501293
34. Cawthorn RG, Eales HV, Walraven F, Uken R, Watkeys MK (2006) The Bushveld Complex. In: Johnson MR, Anhaeusser AC, Thomas RJ (eds) The geology of South Africa. Geological Society of South Africa, Johannesburg/ Council for Geoscience, Pretoria, pp 261–282
35. Minerals Council of South Africa, 2022. Platinum. Online at: https://www.mineralscouncil.org.za/sa-mining/platinum
36. Wilson A (1996) The Great Dyke of Zimbabwe. Dev Petrol 15:365–402
37. Gautam, T.P. (2018). Cohesive soils. In: Bobrowsky, P.T., Marker, B. (eds) Encyclopedia of engineering geology. Encyclopedia of Earth Sciences Series. Springer, Cham. https://doi.org/10.1007/978-3-319-73568-9_60
38. Keaton, J.R. (2018). Noncohesive soils. In: Bobrowsky, P.T., Marker, B. (eds) Encyclopedia of engineering geology. Encyclopedia of Earth Sciences Series. Springer, Cham. https://doi.org/10.1007/978-3-319-73568-9_212
39. Swart D, Dippenaar MA, Van Rooy JL (2023) Field tests for the identification of silts. Bull Eng Geol Env 82:425. https://doi.org/10.1007/s10064-023-03442-7
40. SANS 3001-GR1 (2010) Ed. 1.1. South African National Standard. Civil engineering test methods. Part GR20: determination of the moisture content by oven-dryings. SABS Standards Division. Pretoria
41. Van der Merwe DH (1964) The prediction of heave from the plasticity index and the percentage clay fraction of soils. S Afr Inst Civ Eng 6:103–107
42. SANS 3001-GR20 (2010) Ed. 1.1. South African National Standard. Civil engineering test methods. Part GR20: determination of the moisture content by oven-drying. SABS Standards Division. Part GR10: determination of the one-point liquid limit, plastic limit, plasticity index and linear shrinkage
43. SANS 3001-GR10 (2013) Ed. 1.2. South African National Standard. Civil engineering test methods. SABS Standards Division. Pretoria
44. SANS 3001-PR5 (2011) Ed 1.1. South African National Standard. Civil engineering test methods. Part PR5: computation of soil-mortar percentages, coarse sand ratio, grading modulus and fineness modulus. SABS Standards Division. Pretoria

45. SANS 5844–2 (2014) Ed 2.2. South African National Standard. Particle and relative densities of aggregates. SABS Standards Division. Pretoria
46. AASHTO T 180 - standard method of test for moisture–density relations of soils using a 4.54-kg (10-lb) rammer and a 457-mm (18-in.) drop | globalspec. Available at: https://standards.globalspec.com/std/14316821/aashto-t-180 (Accessed: 05 June 2024)
47. ASTM D2487–17e1. [last update 2020] Standard practice for classification of soils for engineering purposes (Unified Soil Classification System). ASTM International, West Conshohocken

Publisher's Note Springer Nature remains neutral with regard to jurisdictional claims in published maps and institutional affiliations.